



5-2017

Impact of Transportation Infrastructure on Stream Water Quality: Contribution from Stormwater Runoff

Andrew James Steinman

University of Tennessee, Knoxville, asteinma@vols.utk.edu

Follow this and additional works at: https://trace.tennessee.edu/utk_gradthes

 Part of the [Environmental Engineering Commons](#)

Recommended Citation

Steinman, Andrew James, "Impact of Transportation Infrastructure on Stream Water Quality: Contribution from Stormwater Runoff. " Master's Thesis, University of Tennessee, 2017.
https://trace.tennessee.edu/utk_gradthes/4719

This Thesis is brought to you for free and open access by the Graduate School at TRACE: Tennessee Research and Creative Exchange. It has been accepted for inclusion in Masters Theses by an authorized administrator of TRACE: Tennessee Research and Creative Exchange. For more information, please contact trace@utk.edu.

To the Graduate Council:

I am submitting herewith a thesis written by Andrew James Steinman entitled "Impact of Transportation Infrastructure on Stream Water Quality: Contribution from Stormwater Runoff." I have examined the final electronic copy of this thesis for form and content and recommend that it be accepted in partial fulfillment of the requirements for the degree of Master of Science, with a major in Environmental Engineering.

Qiang He, Major Professor

We have read this thesis and recommend its acceptance:

Kimberly Carter, John S. Schwartz, Jon M. Hathaway

Accepted for the Council:

Dixie L. Thompson

Vice Provost and Dean of the Graduate School

(Original signatures are on file with official student records.)

Impact of Transportation Infrastructure on Stream Water Quality: Contribution from Stormwater Runoff

A Thesis Presented for the
Master of Science
Degree
The University of Tennessee, Knoxville

Andrew James Steinman
May 2017

Copyright © 2016 by Andrew J. Steinman

All rights reserved

Acknowledgements

I would like express my deepest gratitude to my major professor, Dr. Qiang He for his expertise, guidance, and commitment throughout this project. His mentorship and support has been utterly invaluable to me. I also thank my committee members, Dr. Carter, Dr. Hathaway, and Dr. Schwartz for their continuous support, input, and knowledge. I would also like to thank my family and friends for their encouragement, love, and support throughout the pursuit of my degree. Lastly, I'd like to thank Landra Phillips for being by my side throughout my seemingly infinite schooling. She was always there to lift my spirits when I would hit roadblocks in my research and convince me that giving up is never the answer.

Abstract

Stormwater runoff is a vital concern to the health of natural waterbodies and ecosystems within urban watersheds. While there is already ample research dedicated to understanding water quality from urban roadways, few of those studies have focused on measuring the dynamics of how stream water quality during storm conditions changes due to increased pollutant load from major urban roadways. With the goal to develop effective water resource management strategies for an impaired tributary watershed, water quality was monitored at four locations within a subwatershed to determine what impact pavement runoff of a major interstate has on the impaired receiving stream. Flow-weighted composite samples of suspended solids, nutrients, and indicator microorganisms were taken along the receiving stream before and after the input of runoff from the interstate. Roadway stormwater runoff was sampled from the pavement as well as from the grassy swale along the interstate roadway.

Table of Contents

Part 1: Introduction	1
Part 2: Methods and Materials	5
Region Specifics	5
Site Selection	7
Site Description.....	7
Monitoring Stations	7
Station SC1	9
Station SC2	9
Station RO1.....	10
Station RO2.....	10
Station RO3 (not used).....	11
Sampling Design.....	12
Water Sample Collection	12
Flow Monitoring	13
Sample Collection Period	13
Laboratory Methodology	14
Pollutant Concentration Calculation	15
Determination of mass-based pollutant loading	16
Data Analysis	17
Part 3: Results	19
Objective A: Overall variation in water quality concentrations among each site within the watershed	19
Rainfall Characteristics	19
Descriptive statistics of water quality constituent.	19
Objective B: Relationship of rainfall and flow characteristics on water quality at each site ...	26
Storm Type Cluster Analysis	26
Seasonal Analysis	26
Correlation Analysis	31
Objective C: Determination of relative contribution of pollutant loading from the roadway ..	34
Contribution of TSS from interstate roadway runoff (Road).....	34
Contribution of TSS from upstream (SC1)	36

Contribution of fecal indicator from roadway runoff (Road)	36
Contribution of fecal indicator from upstream (SC1)	38
Contribution of nitrogen from roadway runoff (Road)	39
Contribution of nitrogen from upstream (SC1)	40
Part 4: Discussion	41
Relative Contribution.....	41
Impact of location	43
Part 5: Conclusion.....	45
References	46
Appendices.....	49
Appendix A, Chemical and hydrological characteristics at each site	50
Appendix B, Site photos	58
Appendix C, Laboratory methodology	63
pH.....	63
Suspended Solids	63
Indicator Microorganisms	64
Nutrients.....	65
Vita.....	68

List of Tables

Table 2.1. Stream and Highway runoff constituents.	14
Table 3.1. Characteristics of 26 rainfall events from March, 2014 to November, 2014.	20
Table 3.2. Criteria of total precipitation (P_t) and 5-min. maximum rain intensity ($I_{\max 5}$) for the classification of storm type (ST).	22
Table 3.3. Summary statistics of water quality constituents for locations RO1, RO2, SC1, and SC2. CV=coefficient of variation.	23
Table 3.4. Explanatory variables utilized in correlation analyses.	32
Table 3.5. Spearman rank correlation coefficients between water quality concentrations.	33
Table 3.6. Spearman's rank correlation coefficients between water quality concentrations and explanatory variables.	33
Table 3.7. TSS loading and relative contribution from interstate roadway stormwater runoff (Road) to receiving stream (SC2).	35
Table 3.8. TSS loading and relative contribution from upstream (SC1) to receiving stream (SC2).	37
Table 3.9. Fecal coliform loading and relative contribution from interstate roadway stormwater runoff (Road) to the receiving stream (SC2).	37
Table 3.10. Fecal coliform loading and relative contribution from upstream (SC1) to the receiving stream (SC2).	38
Table 3.11. $\text{NO}_{2+3}\text{-N}$ loading and relative contribution from interstate roadway stormwater runoff (Road) to the receiving stream (SC2).	39
Table 3.12. $\text{NO}_{2+3}\text{-N}$ loading and relative contribution from upstream (SC1) to the receiving stream (SC2).	40
Table A.1. Physical and chemical characteristics of water samples at site RO1.	50
Table A.2. RO1 rainfall and flow characteristics.	51
Table A.3. Physical and chemical characteristics of water samples at site RO2.	52
Table A.4. RO2 rainfall and flow characteristics.	53
Table A.5. Physical and chemical characteristics of water samples at site SC1.	54
Table A.6. SC1 rainfall and flow characteristics.	55
Table A.7. Physical and chemical characteristics of water samples at site SC2.	56
Table A.8. SC2 rainfall and flow characteristics.	57

List of Figures

Figure 2.1. The receiving watershed in light grey, Knoxville, TN. The dark grey section represents the catchment area sampled in this study. The blue line represents the receiving stream.	6
Figure 2.2. Location of monitoring sites. The shaded area designates the portion of the subwatershed draining at SC1, which is upstream of the road runoff entry points (RO1 and RO2). The road section in red designates the segment of the interstate roadway that contributes stormwater runoff to the subwatershed (area surrounded by the black border line) which drains to the receiving stream at monitoring site SC2.	8
Figure 2.3. Locations of stormwater monitoring sites RO1 and RO2. The blue line indicates the receiving stream bed. RO1 (area indicated by solid black outlined in white) was used to monitor stormwater runoff from the interstate only. RO2 (area outlined in black) was used to monitor stormwater runoff from both the interstate roadway and local traffic that passes under the interstate overpass.	11
Figure 3.1. Dendrogram tree diagram of the total 26 storms by hierarchical cluster analysis categorizing four different storm types (ST).	21
Figure 3.2. Scatterplot highlighting four storm types (ST). P_t =total precipitation on x-axis, $I_{\max 5}$ =5-minute maximum rain intensity on y-axis.	21
Figure 3.3. Spatial progression of TSS and VSS concentration of rainfall events throughout the sampling period at site SC1.	24
Figure 3.4. Significant differences among TSS (a) and VSS (b) concentrations among each sampling site by season. Spring sampling did not occur at site SC2. Within a site, seasons that share similar lower case letters are not significantly different from one another at a 0.05 level according to the Wilcoxon rank sum test. Throughout this table, the largest means are always denoted by “a” and get smaller with each consecutive letter. Error bars represent standard deviation.	28
Figure 3.5. Significant differences among Total Coliform (a) and Fecal Coliform (b) concentrations among each sampling site by season. Spring sampling did not occur at site SC2. Within a site, seasons that share similar lower case letters are not significantly different from one another at a 0.05 level according to the Wilcoxon rank sum test. Throughout this table, the largest means are always denoted by “a” and get smaller with each consecutive letter. Error bars represent standard deviation.	29
Figure 3.6. Significant differences among $\text{NO}_{2+3}\text{-N}$ (a), SO_4 (b), and O-PO_4 (c) concentrations among each sampling site by season. Spring sampling did not occur at site SC2. Within a site, seasons that share similar lower case letters are not significantly different from one another at a 0.05 level according to the Wilcoxon rank sum test. Throughout this table, the largest means are always denoted by “a” and get smaller with each consecutive letter. Error bars represent standard deviation.	30
Figure 4.1. Distribution of TSS loading to the receiving stream (SC2).	42
Figure 4.2. Distribution of fecal coliform loading to the receiving stream (SC2).	42
Figure 4.3. Distribution of Nitrite plus nitrate loading to the receiving stream (SC2).	43
Figure B.1. Site RO2 security box, rain gage, and solar panel.	58
Figure B.2. Site SC1 sampling point.	59
Figure B.3. Site SC1 sampling point looking upstream through conveyance tunnel.	60
Figure B.4. Site SC2 sampling point.	61
Figure B.5. Site SC2, sampling point looking upstream.	62

Figure C.1. Nitrite calibration curve.	66
Figure C.2. Nitrate calibration curve.	66
Figure C.3. Ortho-phosphate calibration curve.....	67
Figure C.4. Sulfate calibration curve.	67

Part 1: Introduction

Urban stormwater discharge during wet weather flow is a major contributor to the pollution of many receiving waters (Appel & Hudak 2001; Brezonik & Stadelmann 2002; Buffleben et al. 2002). As part of the urbanization process, highways have become a potential source for an extensive variety of contaminants to surface and subsurface waters (Mitton and Payne, 1997, Barrett et al., 1995, Gupta et al., 1981). Urban growth has several detrimental impacts on receiving waters. It increases the impervious land area in a region, which decreases infiltration, increases runoff, and decreases the time during which runoff occurs. Moreover, the effects of urban runoff on receiving water quality are highly site-specific (Brezonik and Stadelmann, 2002; USEPA, 1983; Withers and Jarvie, 2008), making it difficult to predict impacts and design appropriate management and control practices without site-specific data.

The 2004 reporting cycle of the US EPA's National Water Quality Inventory Report to Congress indicated that 246,002 miles of rivers and streams as being impaired, or not supporting one or more of their designated uses (USEPA, 2009). Dominate causes of impairment for the assessed rivers and streams were pathogens, which indicate possible fecal contamination that may cause illness in people; habitat alteration, such as disruption of stream beds and riparian areas. The report states the top leading source of impairment of streams is agricultural activities, such as crop production, grazing, and animal feeding; other leading sources included municipal discharges/sewage and urban runoff/stormwater. Non-point sources of fecal coliform loading may be potentially attributable to factors stemming from urban development. Multiple sources include stormwater runoff, leaks and overflows from sanitary sewer systems, runoff from improper disposal of waste materials, leaking septic systems, and domestic animals.

Rivers and streams carry sediment loads in their natural state, but suspended solids become considered a pollutant when they significantly exceed natural concentrations and have a detrimental effect on the water quality (FHWA, 2001). Nonpoint sources of sediment loading to the receiving streams include natural erosion from the weathering of soils, rocks, and uncultivated land; urban erosion from bare soil areas under construction and wash-off of accumulated street dust and litter from impervious surfaces; and erosion from unpaved roadways (TDEC, 2005). High sediment loads increase the probability of transporting nutrients, organic constituents, and microbial forms that may be attached to the particles (Irish et al., 1995). Past research has found strong correlations between fecal coliforms and total suspended solids concentrations (Mallin et al. 2009).

Stormwater runoff that carries increased concentrations of nitrogen and phosphorous is undesirable because these pollutants can stimulate algal bloom in receiving waters. In urbanized areas, the high impervious surface coverage exacerbates the runoff of nutrients from lawns, gardens, and landscaped areas by increasing the “flashiness” or erratic and rapid inputs of runoff into creeks (Holland et al. 2004) and providing a rapid conduit for nutrients and other pollutants to enter receiving waters. Nonpoint sources of nitrogen include natural sources such as mineralization of soil organic matter, atmospheric deposition, animal waste, and fertilizers (FHWA, 2001).

Ortho-phosphate is the most common inorganic form of phosphate and a potential pollutant to surface waters due to its stimulation of bacteria (Mallin et al. 2004). Percent of urban development and impervious surface were positively correlated with orthophosphate in the three watersheds studied, suggesting a combination of anthropogenic sources of orthophosphate in these watersheds and increased delivery efficiency to surface waters.

Hoffman et al. (1985) found that concentrations of various pollutants in highway runoff varied within the storm event and that, in general, peaks in pollutant concentrations occur during high flow rates when transport of contaminants is more efficient. However, peak concentrations may occur during lower flow conditions, due to reduced dilution. Higher concentrations of pollutants are often observed during the first runoff from a storm, often described as “first-flush” (Barrett et al. 1995).

Season and weather conditions may have a large impact on highway pollutant concentrations. Helmreich et al. (2010) witnessed a considerable seasonal increase in pollutant concentrations such as suspended solids and pH during the cold season. The mean values during winter time were multiple times higher than measured during the warm season.

Water quality samples are analyzed for “indicator organisms” that signify the potential presence of pathogens that potentially are responsible for waterborne diseases such as typhoid and paratyphoid fever, dysentery, diarrhea, and cholera, have been observed in highway runoff (Sartor et al., 1974; Gupta et al. 1981). While no point sources of fecal coliform loading were documented in the watershed, the non-point sources may be potentially attributable to factors stemming from urban development. Multiple sources including stormwater runoff, leaks and overflows from sanitary sewer systems, runoff from improper disposal of waste materials, leaking septic systems, and domestic animals (TDEC, 2005).

The overall goal of this study was to investigate the role of the water quality in stormwater runoff from a major interstate roadway contributes to the local receiving waterbody. Specific objectives were (a) monitor the concentration and loads of suspended solids, nutrients, and fecal indicator organisms at four sub-catchments within the receiving watershed, (b) determine relationships between runoff water quality and characteristics of storm events, and (c)

determine the relative contribution of pollutant loading to the receiving waterbody, with a focus on the mass-based loading of total suspended solids (TSS), nitrite plus nitrate as nitrogen ($\text{NO}_{2+3}\text{-N}$), and fecal indicators (FC). Focus is given to these pollutants as these have a history of contributing to the impairment of the local receiving waterbody (TDEC, 2005; TDEC, 2014). Mass-based pollutant loading eliminates biases arising from disregarding stormwater quantity, thus superior to concentration-based parameters. However, typical stormwater monitoring programs target the concentrations of pollutants only. This study aims to develop a stormwater runoff monitoring methodology for the determination of mass-based pollutant loading to support the prioritization of potential mitigation efforts to reduce the waterway's loading to levels below the designated TMDL of each pollutant.

Part 2: Methods and Materials

Region Specifics

The receiving watershed (**Figure 2.1**) has an area of 6.27 mi² with a stream length of 12.8 miles. The stream is a tributary of the Tennessee River and flows approximately north to south, confined by two other tributary watersheds on its east and west border. The topography of the watershed in this study is characterized by mostly rolling ridges and valleys. The region has a humid subtropical climate with regular periods of below freezing temperatures in winter. Air temperature in ranges from an average January low of 38° F to an average high of 78° F in July. In the average year, there is 47.9 inches of total rain, 6.5 inches of snow, and 125 wet days (NWS, 2014). Approximately 51% of the land in the is used for residential land purposes, compared to 22 % for commercial and industrial uses. Forest covers 24% while agricultural land uses occupy 3%. The watershed was found to be approximately 41% urban.

In the last 20 years, the local municipality has seen significant increase in urban development, resulting in extensive degradation of its surrounding watersheds. In the recent years, the watershed was added to the Tennessee Department of Environment and Conservation's 303(d) list for impaired waterways. The 303(d) list, which is required by the federal Clean Water Act, is a compilation of the lakes, rivers, and streams in Tennessee that fail to meet one or more water quality standards. The receiving watershed in this study was added due to high pathogen levels associated with urban stormwater runoff and collection system failure, and for inability to support its designated use classification due for siltation/habitat alteration associated with urban runoff, land development, and bank modification. Designated use classifications for the receiving stream include the ability to support fish and aquatic life, recreation, irrigation, livestock watering and wildlife, and industrial water supply (TDEC, 2014).

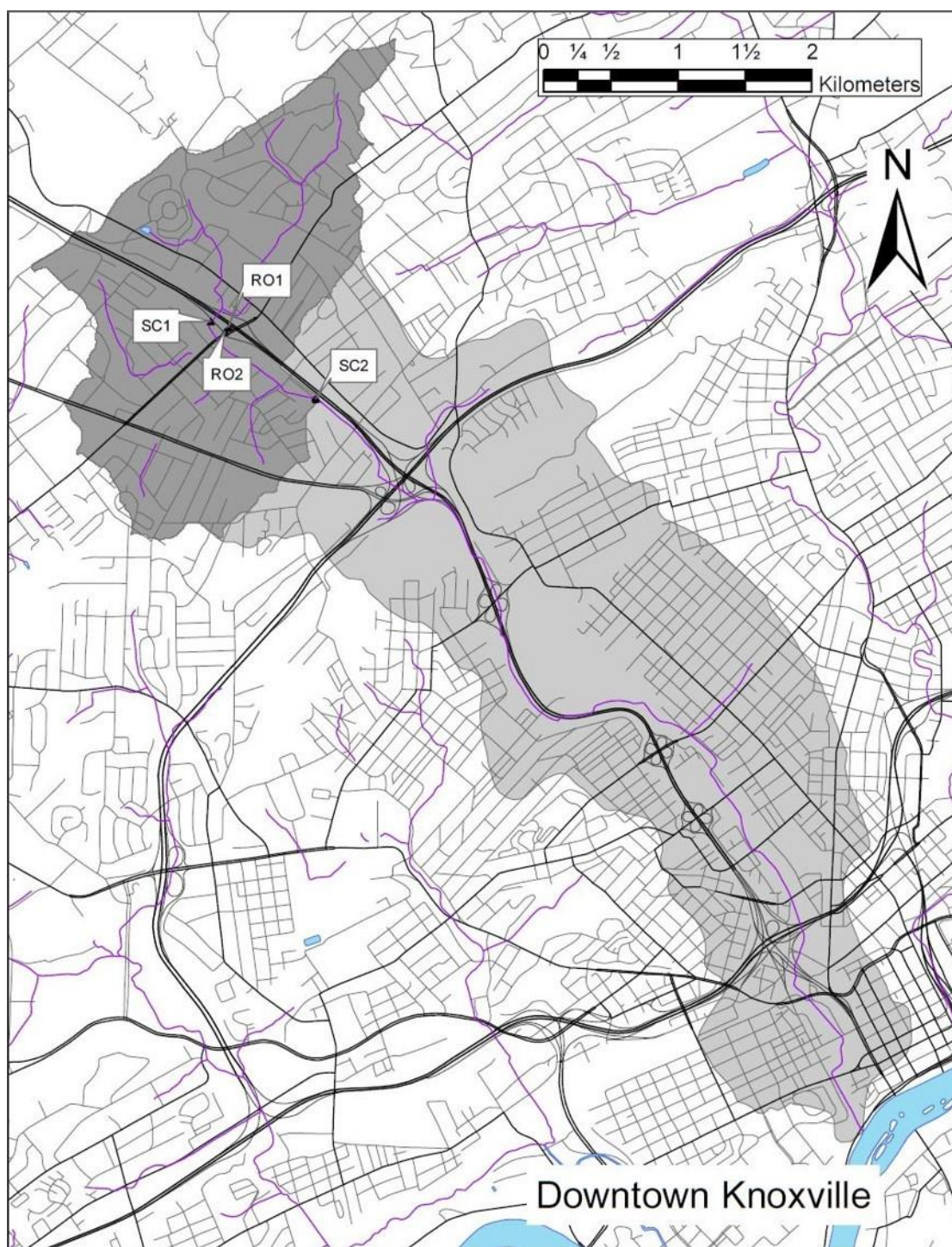


Figure 2.1. The receiving watershed in light grey, Knoxville, TN. The dark grey section represents the catchment area sampled in this study. The blue line represents the receiving stream.

Site Selection

Site selection involved identifying a point along an impaired urban watershed with as little distance as possible between the stream and source of roadway runoff. This location was selected due to the close proximity of an impaired receiving stream to an interstate highway.

Site Description

The data for this study is collected within upper region of impaired watershed, centralized at intersection of a local road system and a U.S. interstate roadway as shown in **Figure 2.1**. At this location, the flow of the receiving stream travels west underneath the interstate right-of-way via a 10-ft rectangular concrete channel. The interstate roadway consists of 6 lanes in total with north- and south bound traffic separated by a concrete barrier. Runoff from the innermost lane drains to drop inlets at the dividing barrier where it is piped to a grassy slope just beyond the shoulder of the roadway. Runoff from the outermost lane drains to the shoulder and flows directly off the roadway surface to the grassy swale. Concrete conveyance ditches located on either side of the interstate direct stormwater runoff to the receiving stream. Within the northern grassy swale portion of the interstate right-of-way, bordered by the exit ramp and interstate, a simple network of concrete swales direct flow to a central drainage point where it meets with the receiving stream.

Monitoring Stations

Primary tasks of this project included the monitoring and analysis of pollutant loading in stormwater runoff from transportation systems. Four sampling sites were monitored with ISCO automatic samplers (**Figure 2.2**). Stream samples are taken at two points along the receiving stream, one upstream of the roadway sampling point and one downstream, labeled SC1 and SC2

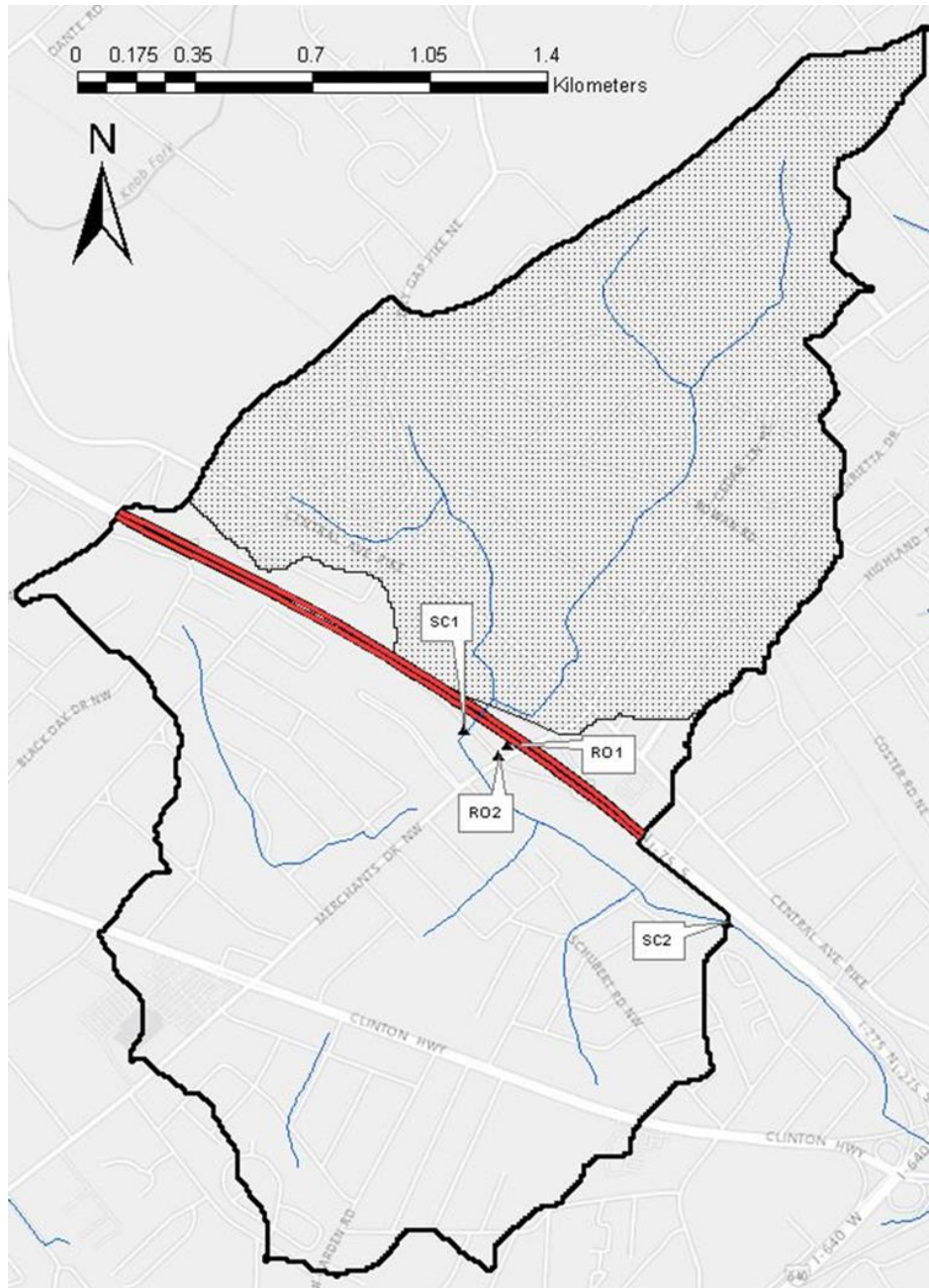


Figure 2.2. Location of monitoring sites. The shaded area designates the portion of the subwatershed draining at SC1, which is upstream of the road runoff entry points (RO1 and RO2). The road section in red designates the segment of the interstate roadway that contributes stormwater runoff to the subwatershed (area surrounded by the black border line) which drains to the receiving stream at monitoring site SC2.

respectively. Roadway sampling was initially taken at three points within the interstate right-of-way, labeled RO1, RO2, and RO3, however, site RO3 was removed midway through the study due to equipment malfunctions.

Station SC1

Station SC1 was deployed to monitor and sample the receiving stream flow upstream of the entry point of stormwater runoff from the interstate right-of-way during storm events (**Figure 2.2**). SC1 was also used to determine the pollutant loading transported by the stream flow itself prior to the input of stormwater from the interstate roadway.

Site SC1 is located at the west end of the rectangular concrete conveyance channel. The channel dimensions are documented as 10-ft x 6-ft x 491-ft. A shallow bed of coarse sediment lined the bottom of channel throughout its length and near the exit the walls of the channel were caked with a silty debris (**Appendix B, Figure B-2**). To ensure accurate sampling, samples were taken at a point (approx. 20-ft inside) where no natural alterations were made to the channel walls.

Station SC2

The SC2 sampler was deployed to monitor and sample the receiving stream flow downstream of the entry point of stormwater runoff from interstate right-of-way during storm events SC2 was used to determine the pollutant loading after the input of stormwater from the interstate roadway.

Site SC2 was chosen approximately 1 km downstream of SC1 to accommodate any flow originating from site RO3 (**Figure 2.2**). At this location, the receiving stream has a much larger flow (**Appendix B, Figure B-5**). The catchment area for the downstream site is 5.10 km² while the upstream catchment area is 2.40 km² or 47% of the watershed of the site. Land use in

downstream portion of the watershed is 70% residential, with 38% residing within the upstream catchment area. Commercial land use comprises 27% of total catchment area, 7% of which is in the upstream catchment. Approximately 29% of the downstream catchment is covered in paved surface, with 10% within the upstream portion of the catchment basin.

Station RO1

Station RO1 was deployed to monitor stormwater runoff exclusively from the pavement of the interstate in the subwatershed (**Figure 2.3**). RO1 was intended to determine the pollutant loading in stormwater runoff originated from the interstate.

Samples from the RO1 site are taken as close to the road surface itself via a stormwater drop-inlet outfall. RO1's catchment area encompasses approximately 3,000 m² of roadway, all impervious, collecting from the north-bound traffic lanes. At its discharge point, the RO1 stormwater runoff is directed down the slope of the elevated roadway following a slightly curved concrete paved ditch where it immediately drains into the second sampling point, RO2.

Station RO2

Station RO2 was deployed to monitor stormwater runoff from the interstate and the grassy swale area within the interstate right-of-way (**Figure 2.3**). Station RO2 was not used to determine the relative loading from the interstate roadway due to the influence the grassy swale area might have on the results. Our focus was on loading from the pavement only.

RO2 is located on the far western side of the interstate right-of-way along the west-bound local traffic where all runoff within the grassy portion of the interstate right-of-way converges through a single 24-inch MS4 pipe discharging immediately to the receiving stream. RO2 has a catchment area of approximately 31,600 m², of which 15,600 m² is interstate roadway. See **Appendix B, Figure B-1** for a site photo.

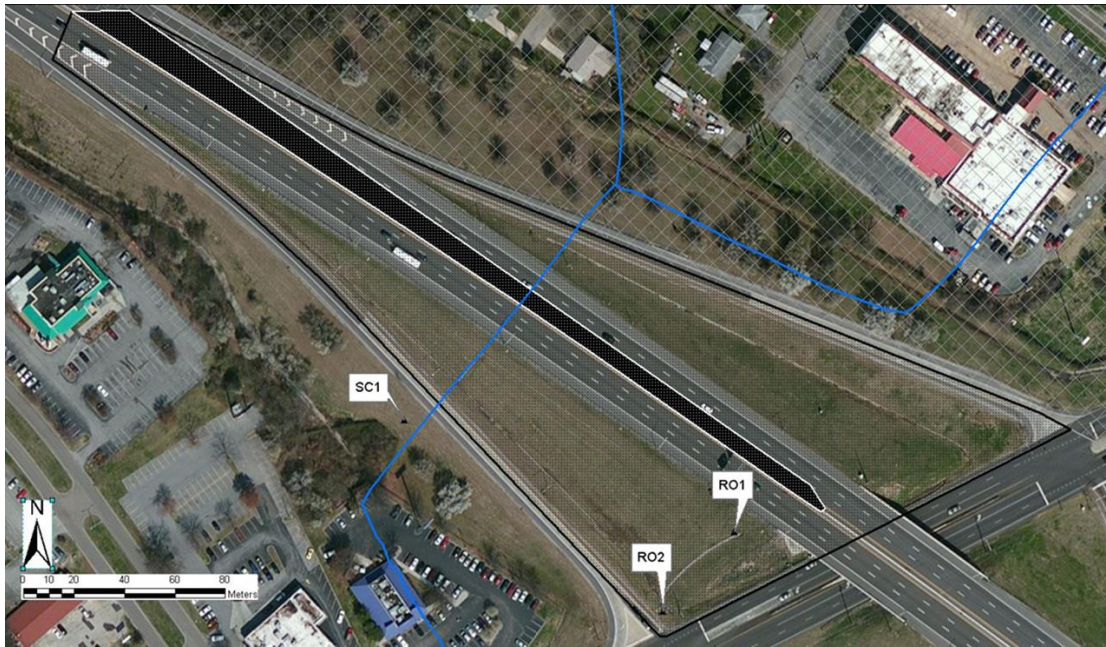


Figure 2.3. Locations of stormwater monitoring sites RO1 and RO2. The blue line indicates the receiving stream bed. RO1 (area indicated by solid black outlined in white) was used to monitor stormwater runoff from the interstate only. RO2 (area outlined in black) was used to monitor stormwater runoff from both the interstate roadway and local traffic that passes under the interstate overpass.

Station RO3 (not used)

Site RO3 was installed across the street from RO2 directly next to a catch basin at the lowest elevation point in the grassy area bordered by the on-ramp leading to the interstate and the local roadway that passes under the interstate overpass. The drainage area of RO3 spanned the grassy areas east and west of the interstate to the entrance and exit ramp on the southern side of the street. The catch basin drained influent stormwater through a 1.5-foot diameter pipe that leads underneath the interstate on-ramp where it discharges to a grassy ditch and wetland area before it reaches the receiving stream.

For unknown reasons, equipment malfunctions were rampant at site RO3. From March, 2014 when sampling began until early August, 2014, the autosampler captured a successful,

complete storm event only three times. In August, the decision was made to cease collection at site RO3 and remove all data collected at that site from the research project.

Sampling Design

Water Sample Collection

Automatic flow measuring and sampling systems were installed and operated at five locations within the watershed. Water quality samples were collected during runoff events at each location within the site with an ISCO 6712 automatic sampler equipped with Teflon sampling tubing and silicone peristaltic pump tubing. Water levels at each location were measured using ISCO 750 area velocity flow meters.

Each sampling station included a 12-volt battery to power the flowmeter and sampler. A solar panel (SunWize OEM 40) recharged the battery. The sampler, flowmeter module, and battery were housed in a large steel enclosure (**Appendix B, Figure B-1**). Sampling protocol for each storm event was initiated by a rain gauge when rainfall volume exceeded 0.06 inches within 3 hours. Rainfall was measured at each site using an ISCO Model 674 rain gauge equipped with a “tipping bucket” that measures rainfall in 0.01 inch increments hyetograph was recorded in 1-minute intervals throughout the duration of a storm event. Note that while each site was equipped with its own rain gauge, for simplicity only the RO2 rain gauge data was used for analysis during a rainfall event, save two events in which RO2 was out of order and did not collect any rainfall data.

Samplers were configured with eight, 1.8-liter glass bottles and programmed to collect multiple flow-weighted composite samples per bottle. Prior to a storm event the bottles were rinsed with distilled water to reduce contamination. Flow pacing and sampling distribution per

bottle was adjusted prior to a storm event to allow an adequate characterization of the storm with a minimum of five samples per storm. Samples were kept on ice in the field until transferred to the laboratory. The information recorded at the automatic sampling station included rainfall volume and intensity; runoff liquid level and velocity; and sampling times. Data was recorded in 1-minute intervals and downloaded from the sampler to a proprietary transfer device (ISCO 581) and uploaded to desktop computer where it was converted to text format, and exported to Microsoft Excel.

Flow Monitoring

Flow rate conversion is determined by measuring level, velocity, and cross-sectional area of the channel. A sensor probe placed in the channel flow path measures both liquid level and velocity. An internal differential pressure transducer located on the bottom of the probe converts hydrostatic pressure to liquid level. A second pair of ultrasonic transducers located within the probe measure velocity through the utilization of ultrasonic sound waves and the Doppler effect. For sites RO1, RO2, RO3, and SC1, cross-sectional area is determined using programed channel dimensions. At site SC2 the channel is irregularly shaped which required the input multiple level-to-area data points into the auto sampler to calculate flow rate.

Sample Collection Period

Sampling stations were installed in mid-January 2014. Sample collection did not begin until mid-March, 2014 (except for the autosampler at site SC2, which was installed later) due to the time needed to troubleshoot and replace/repair non-working equipment, as well as test the sampling and laboratory methods. Sampling for all sites continued until mid-November, 2014. Sampling station SC2 remained out of order to swap non-working parts at other sampling sites until replacements arrived. SC2 endured further complications in mid-February, 2014 when the

pre-approved sampling location needed to be moved further downstream. The sampler moved to its current location in early-March, 2014. Sampling collection was delayed until mid-June, however due in part to: 1.) time needed to ship additional equipment required by the new site, and 2.) repair-time of multiple equipment malfunctions that took place once the autosampler was prepped.

Laboratory Methodology

Total and Fecal coliform counts were determined using Standard Methods 9222 with the M-FC medium (APHA, 2005). An Ion Chromatograph (IC) system (Dionex AS-AP, ICS-2100, ICS-1100) was used for nutrient analysis following Standard Methods 4110 (APHA, 2005).

Total suspended solids (TSS) and volatile suspended solids (VSS) were measured using Standard Methods 2540 (APHA, 2005). Nutrient EMCs found to be below the detection limit of the IC were set equal to one-half of the respective detection limit as indicated in **Table 2.1**. A detailed summary of laboratory methods is located in **Appendix C**.

Water quality analysis was performed on average within 8 hours of sampling initiation and always within 24 hours after the start of each storm event. Water quality analysis included

Table 2.1. Stream and Highway runoff constituents.

Lab Analysis	Detection Limit
Suspended Solids	
TSS	1 mg/L
VSS	1 mg/L
Nutrients	
NO ₂₊₃ -N	15 µg/L
O-PO ₄	6 µg/L
SO ₄	11 µg/L
Microbial	
Total coliform	1 CFU/100 mL
Fecal coliform	1 CFU/100 mL

measurements of pH, nutrients, fecal coliform, and suspended solids. Concentration is reported in milligrams per liter (mg/L) or micrograms per liter (µg/L) apart from bacteria counts which are reported in “colony-forming units” per 100 mL (CFU/100 mL).

Pollutant Concentration Calculation

The event mean concentration (EMC) as described by Lee et al. (2002) can be interpreted as a flow-weighted average of pollutant concentrations of a storm event. The EMC is defined as the total constituent mass discharged during an event divided by the total volume of discharge during the event (Huber & Maidment 1992), given as:

$$EMC = \frac{M}{V} = \frac{\int C(t)Q(t)dt}{\int Q(t)dt} \quad (\text{Equation 1})$$

For this study, a single composite sample for each site was achieved using the following method:

1.) Each 1.8-liter glass sample bottle containing a flow-weighted sub-composite sample of a storm event was carefully shaken to resuspend particulate matter and poured into a sterilized 300-ml, screw top, polypropylene containers used for transport.

2.) The labeled 300-ml samples were chilled in a cooler and transported to the Department of Civil and Environmental Engineering at University of Tennessee for immediate analysis.

3.) Composite samples for each site were created by transferring a fixed amount from each transport container into a clean glass laboratory beaker to create a single flow-weighted composite sample of the storm event. Prior to transferring the sample, the 300-mL bottle of sample water was shaken up to resuspend all solids and ensure the concentration was

representative of the storm event. Prior to transferring the sample, the 300-mL bottle of sample water was shaken up to resuspend all solids and ensure the concentration was representative.

Determination of mass-based pollutant loading

Runoff volume was obtained by summing the discharge measurements from the timestamp of the first sampling point to the timestamp of the last sampling point. Discharge was calculated automatically in 1-minute intervals using runoff liquid level and velocity data provided by the ISCO 750 Area Velocity module.

The mass-based pollutant loading was calculated for each storm event at each monitoring site i as follows:

$$Loading_i = (Concentration_i) \times (Volume_i \text{ of stormwater runoff}) \quad (\text{Equation 2})$$

The relative contribution (RC_i) of pollutant $loading_i$ in the subwatershed was calculated as:

$$RC_i = [(Loading_i) \times (SF_i)] / Loading_{SC2} \quad (\text{Equation 3})$$

where SF_i is the scaling factor for the extrapolation of pollutant $loading_i$ at a particular monitoring site to the entire subwatershed; $Loading_{SC2}$ is the pollutant loading at site SC2 according to Equation 1.

Since site SC1 drains the entire subwatershed upstream of the interstate right-of-way interchange, the SF for SC1 is 1 and no extrapolation is needed. In contrast, RO1 only drains a small segment of the roadway pavement that is in the subwatershed. Therefore, surveying was conducted at the project site to determine the area of the road surface directly drained to RO1

(A_{RO1}). The SF_{RO1} was then calculated by dividing the entire road surface of the interstate ($A_{interstate}$) in the subwatershed by the road surface area directly drained to monitoring site RO1:

$$SF_{RO1} = (A_{interstate}) / A_{RO1} \quad (\text{Equation 4})$$

The relative contribution of the entire interstate roadway within the subwatershed is achieved combining equation 3 and 4. For simplicity, the labeling was changed from RC_{RO1} to “*Road*” to differentiate the loading from site RO1.

$$Road = RC_{RO1} = [(Loading_{RO1}) \times (SF_{RO1})] / Loading_{SC2} \quad (\text{Equation 5})$$

Data Analysis

JMP statistical software was used for data analysis. A two-way cluster analysis was applied to group the 26 storm events into storm type categories based on the magnitude of rainfall characteristic parameters total precipitation and maximum rain intensity.

Water quality EMCs as well as all rainfall and flow characteristic data were checked for normality using histograms and a Kolmogorov-Smirnov test (Hollander and Wolfe, 1999). Most data were found to be lognormally distributed except for ortho-phosphate and pH which did not follow a normal distribution. Since no clearly defined normal distribution was found for all datasets, only nonparametric statistical tests were used to analyze the data. A distribution free Kruskal-Wallis test was used to determine statistical differences in water quality EMCs with two different categorical variables: storm type and season. Constituent concentrations were considered to be significantly different if the chi-square approximation of the Kruskal-Wallis test indicated that the probability of a greater chi square was less than or equal to 0.05. Wilcoxon

rank sum procedure was also utilized to determine significant differences among pollutants through pairwise comparisons.

Using the spearman rank nonparametric analysis, the water quality EMCs were correlated to numerous explanatory variables associated with antecedent climate, precipitation, and hydrologic processes to examine what variables best explained the observed data (as identified by statistically significant correlations). All statistical analyses were performed at an $\alpha=0.05$ significance level unless otherwise noted.

Part 3: Results

Objective A: Overall variation in water quality concentrations among each site within the watershed

Rainfall Characteristics

A total of 26 rainfall events were sampled among the four sites between March 16, 2014 and November 17, 2014. In **Table 3.1**, the rainfall duration, total precipitation, 5-minute maximum rain intensity, average rain intensity, antecedent dry period, as well as storm type classification and ADP classification of each storm event is summarized. All rainfall characteristics were found to follow log-normal distribution. Events 1 and 6 were storms captured that had two separate rainfall occurrences.

The wide range of minimum to maximum values in each column of **Table 3.1** illustrate how no two storms are completely alike. To separate storm events with similar patterns into groups for further study, a cluster analysis was conducted based on the storm characteristic parameters of total rainfall and 5-minute maximum rain intensity. Based on the distances of the branches for each event in **Figure 3.1**, the storm events were grouped into four storm type (ST) categories, labeled ST-1, -2, -3, and -4. A scatterplot shown in **Figure 3.2** illustrates how the storm types differ from one another based on the rainfall characteristics of total precipitation on the x -axis, and 5-minute maximum rain intensity on the y -axis. The boundary condition information of these 4 storm categories are summarized in **Table 3.2**.

Descriptive statistics of water quality constituent.

Though 26 storm events were captured in total, no site had captured all storms through the sampling period. The road runoff sites, RO1 and RO2, captured 21 and 22 storms

Table 3.1. Characteristics of 26 rainfall events from March, 2014 to November, 2014.

Date	Event No.	Season	D_r (hr)	P_t (in)	I_{ave} (in/hr)	I_{max5} (in/hr)	ADP (day)	Storm Type
3/16/14	1	Spring	21.9	0.47	0.06	0.20	13.0	ST-1
3/29/14	2	Spring	3.92	0.19	0.05	0.36	11.1	ST-2
4/27/14	3	Spring	0.92	0.06	0.07	0.12	5.29	ST-2
4/28/14	4	Spring	10.6	1.40	0.13	5.52	0.87	ST-4
4/30/14	5	Spring	1.92	0.18	0.09	0.36	0.83	ST-2
5/14/14	6	Spring	14.5	0.43	0.05	0.36	5.12	ST-1
5/23/14	7	Spring	0.08	0.12	1.44	1.44	7.73	ST-3
5/25/14	8	Spring	0.40	0.10	0.25	0.72	2.34	ST-2
6/04/14	9	Summer	0.45	0.19	0.42	1.56	6.06	ST-3
6/05/14	10	Summer	1.25	0.20	0.16	1.20	0.70	ST-3
6/25/14	11	Summer	1.47	0.20	0.14	0.84	3.41	ST-3
6/29/14	12	Summer	1.00	0.15	0.15	0.60	2.84	ST-2
7/18/14	13	Summer	5.95	0.45	0.08	0.48	9.67	ST-1
7/20/14	14	Summer	1.07	0.14	0.13	0.48	0.66	ST-2
7/27/14	15	Summer	1.68	1.03	0.61	3.96	7.56	ST-4
8/02/14	16	Summer	0.47	1.07	2.28	4.80	5.87	ST-4
8/10/14	17	Summer	1.72	0.23	0.13	0.84	1.98	ST-2
8/20/14	18	Summer	1.35	0.31	0.23	1.44	0.19	ST-3
8/30/14	19	Summer	3.13	0.39	0.12	0.60	10.0	ST-1
9/02/14	20	Fall	3.00	0.24	0.08	0.60	2.86	ST-2
9/11/14	21	Fall	1.87	0.34	0.18	2.04	8.64	ST-3
10/06/14	22	Fall	1.15	0.20	0.17	0.96	3.08	ST-3
10/10/14	23	Fall	4.98	0.26	0.05	0.72	2.28	ST-2
10/14/14	24	Fall	3.77	0.77	0.20	0.96	0.92	ST-1
10/29/14	25	Fall	5.57	0.27	0.05	0.24	13.1	ST-2
11/17/14	26	Fall	8.35	0.74	0.09	0.48	10.4	ST-1
Geometric mean			2.05	0.29	0.15	0.78	3.36	
Mean			3.94	0.39	0.29	1.23	5.25	
Median			1.80	0.25	0.13	0.72	4.26	
Standard deviation			5.02	0.34	0.49	1.40	4.10	
CV			1.27	0.87	1.73	1.14	0.78	
Minimum			0.08	0.06	0.05	0.12	0.19	
Maximum			21.9	1.40	2.28	5.52	13.1	

D_r , rainfall duration; P_t , total precipitation; I_{ave} , average rain intensity; I_{max5} , 5-minute maximum rain intensity; ADP , antecedent dry period.

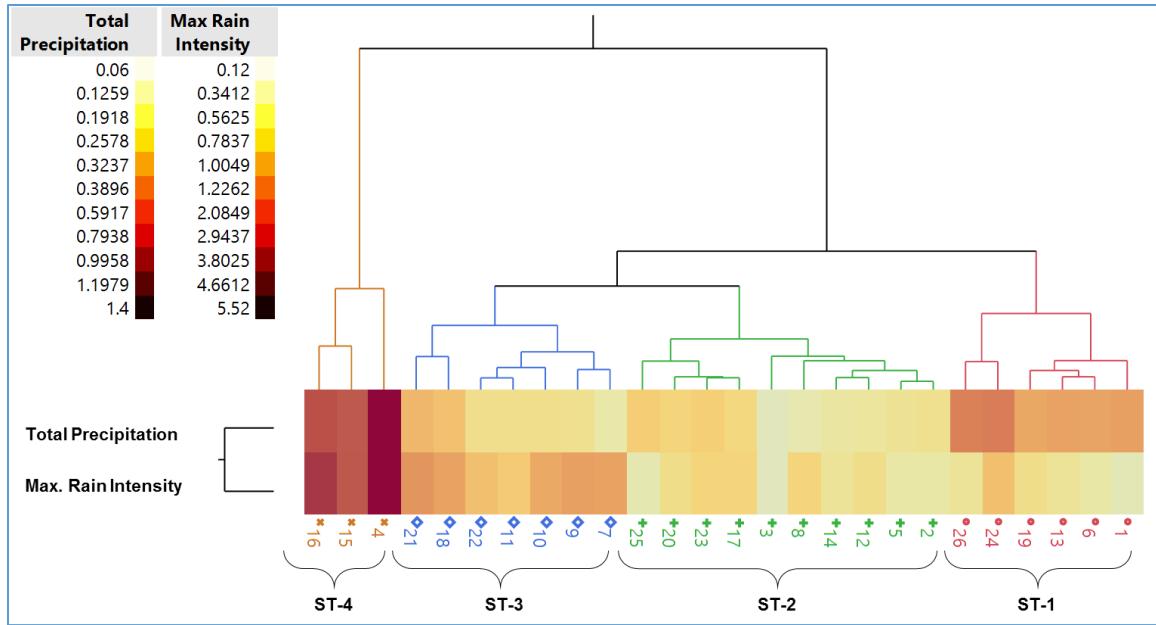


Figure 3.1. Dendrogram tree diagram of the total 26 storms by hierarchical cluster analysis categorizing four different storm types (ST).

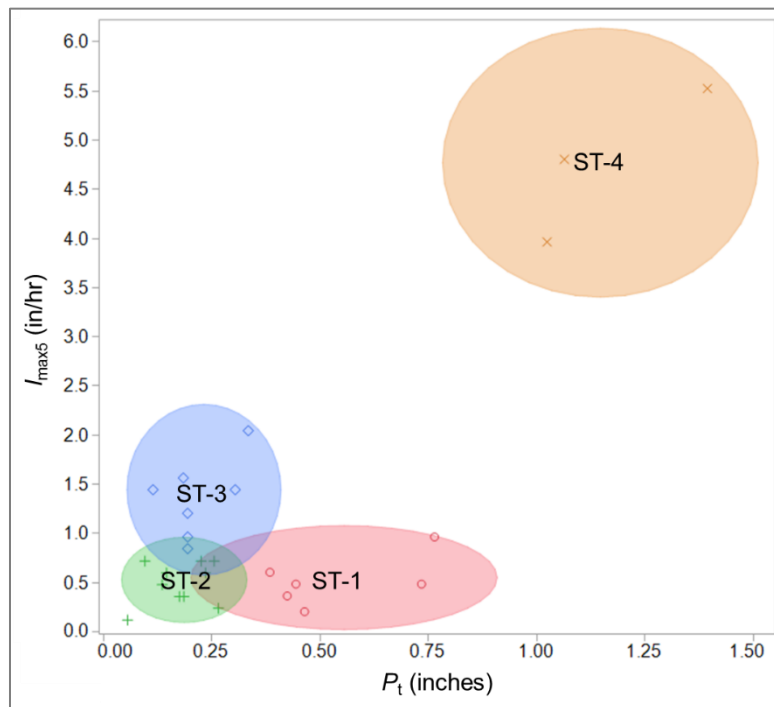


Figure 3.2. Scatterplot highlighting four storm types (ST). P_t =total precipitation on x-axis, $I_{\max 5}$ =5-minute maximum rain intensity on y-axis.

Table 3.2. Criteria of total precipitation (P_t) and 5-min. maximum rain intensity ($I_{\max 5}$) for the classification of storm type (ST).

Classification	Description	P_t (in)		$I_{\max 5}$ (in/hr)	
		Min.	Max.	Min.	Max.
ST-1	moderate precipitation, low peak rain intensity	0.39	0.77	0.20	0.96
ST-2	low precipitation, low peak rain intensity	0.06	0.27	0.12	0.72
ST-3	low precipitation, moderate peak rain intensity	0.12	0.34	0.84	2.04
ST-4	high precipitation, high peak rain intensity	1.03	1.40	3.96	5.52

respectively. The stream sites, SC1 and SC2, captured only 14 and 15 storms, respectively. The event mean concentration (EMC) for each storm event sampled at sites RO1, RO2, SC1, and SC2 is shown in **Table 3.3**. Individual event EMCs for each location as well as flow characteristics may be found in **Appendix A**, in **Table A-1** through **Table A-8**.

The pH levels were more varied in the two roadway sites than at the stream sites. The lowest pH value of 6.79 occurred at site RO2, the highest value reached 8.93 at site RO1 shown in **Table 3.3**. Overall median values for all sites were very close, ranging from 7.76 to 7.90

Total suspended solids across each site ranged from 3.75 mg/L at RO2 to 266 mg/L at SC2. RO1 yielded significantly higher TSS and VSS concentrations compared to RO2 (p -values=0.0168 and 0.0267) for the duration of the study period as determined by matched pair comparison using a nonparametric Wilcoxon signed rank test. This finding provides evidence of a possible mitigating effect the grassy swale has on suspended solids.

Volatile suspended solids (VSS) concentrations were less dynamic throughout the monitoring period and ranged from 1.88 mg/L to 58.8 mg/L, with both minimum and maximum concentrations occurring at site RO2. Median concentrations ranged from 14 mg/L to 21 mg/L.

Comparing TSS and VSS transport variation to one another at each of the four sites, it appears TSS concentrations fluctuate with greater magnitude than VSS concentrations. As both

Table 3.3. Summary statistics of water quality constituents for locations RO1, RO2, SC1, and SC2. CV=coefficient of variation.

Site	Measurement	Volume (m ³)	pH	TSS (mg/L)	VSS (mg/L)	NO ₂₊₃ -N (mg/L)	O-PO ₄ (µg/L)	SO ₄ (mg/L)	Total coliform (CFU/100 mL)	Fecal coliform (CFU/100 mL)
RO1										
	<i>n</i>	21	21	21	21	19	19	12	19	19
	Geometric mean	33	7.80	36.5	17.9	0.41	15.7	6.77	61,897	9,085
	Mean	49	7.82	50.3	21.6	0.55	38.3	7.90	121,737	16,711
	Median	31	7.85	35.7	21.3	0.42	17.1	6.95	78,000	11,000
	Standard deviation	47	0.44	39.6	13.4	0.50	49.8	4.53	166,573	19,090
	CV	0.97	0.06	0.79	0.62	0.90	1.30	0.57	1.37	1.14
	Minimum	2.5	6.93	8.33	5.63	0.09	3.00	2.48	3,000	500
	Maximum	146	8.93	141	56.7	1.96	176	18.8	727,000	67,000
RO2										
	<i>n</i>	22	22	22	22	20	20	20	18	18
	Geometric mean	67	7.74	26.4	14.3	0.48	44.5	9.46	148,791	19,838
	Mean	112	7.75	43.1	19.1	0.64	87.8	10.3	248,222	28,167
	Median	70	7.90	33.1	15.4	0.61	77.8	9.94	180,000	20,000
	Standard deviation	125	0.41	46.8	15.3	0.48	87.1	4.23	227,925	21,639
	CV	1.12	0.05	1.08	0.80	0.74	0.99	0.41	0.92	0.77
	Minimum	7.7	6.79	3.75	1.88	0.06	3.00	3.84	10,000	2,000
	Maximum	451	8.38	189	58.8	1.81	385	18.1	755,000	75,000
SC1										
	<i>n</i>	14	14	14	14	12	12	12	10	10
	Geometric mean	408	7.83	71.0	16.0	0.25	83.6	3.51	178,361	29,789
	Mean	753	7.83	82.9	18.1	0.36	128	3.86	223,700	32,800
	Median	519	7.78	65.4	17.4	0.23	113	3.72	200,500	28,500
	Standard deviation	944	0.26	47.0	8.54	0.34	83.0	1.73	161,697	15,061
	CV	1.25	0.03	0.57	0.47	0.93	0.65	0.45	0.72	0.46
	Minimum	50	7.59	21.9	3.75	0.05	3.00	1.74	60,000	15,000
	Maximum	3,470	8.61	173	38.8	1.09	256	7.31	600,000	60,000
SC2										
	<i>n</i>	15	15	15	15	13	13	13	12	12
	Geometric mean	3,849	7.72	47.9	11.7	0.22	4.91	3.59	30,573	12,787
	Mean	4,794	7.73	73.0	16.2	0.25	10.7	3.80	35,000	14,667
	Median	3,315	7.76	50.0	13.8	0.20	3.00	3.73	34,000	13,000
	Standard deviation	3,613	0.35	72.6	12.5	0.13	19.8	1.28	17,247	7,512
	CV	0.75	0.05	0.99	0.77	0.52	1.85	0.34	0.49	0.51
	Minimum	1,548	6.75	6.67	1.88	0.10	3.00	1.94	8,000	5,000
	Maximum	13,677	8.28	266	50.6	0.48	72.2	6.33	68,000	26,000

pollutants increase over the course of a given storm event, the VSS concentration seems to peak while TSS concentrations continue to increase as the event progresses. An example of this phenomenon is presented in **Figure 3.3**. While many rainfall and environmental variables may influence solids transport dynamics, what remains constant is the limiting behavior of VSS to TSS. This trend indicates there is a limited amount of organic source material in the catchment area available to be washed out.

Nitrite plus nitrate as nitrogen ($\text{NO}_{2+3}\text{-N}$) EMCs ranged from a low of 0.05 mg/L at site SC1 to a maximum of 1.96 mg/L at RO1. Overall, nitrogen concentration was more pronounced in stormwater runoff at sites RO1 and RO2. A matched pair comparison using a Wilcoxon signed rank test indicated a significantly higher concentration of $\text{NO}_{2+3}\text{-N}$ at site RO2 compared to the upstream stream site, SC1 ($p\text{-values}=0.0195$). RO2's nitrogen comparison with downstream site, SC2, was also quite strong, although not strictly statistically significant with a $p\text{-value}$ of 0.0547.

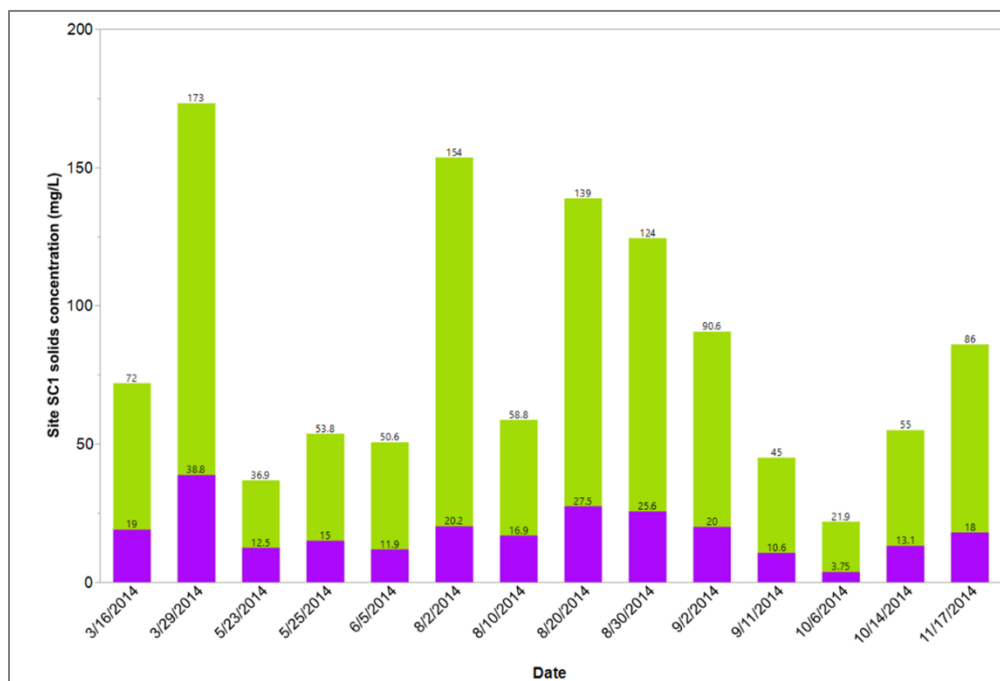


Figure 3.3. Spatial progression of TSS and VSS concentration of rainfall events throughout the sampling period at site SC1.

Ortho-phosphate EMCs were lowest in the downstream site, SC2, where the concentration was below the detection level 10 out of 13 storm events. This finding suggests the possibility of a sink within the SC2 stream bed. Overall ortho-phosphate EMCs were highest at the upstream sampling location, SC1, with a median concentration of 113 µg/L. Next highest median levels of 77.8 µg/L and 17.1 µg/L were found at sites RO2 and RO1, respectively. A non-parametric, matched pair Wilcoxon signed rank test comparing each site confirmed a significantly lower ortho-phosphate concentration at SC2 compared to both the upstream sampling point, SC1, and the grassy area of the interstate catchment, RO2. Coincidentally, both comparisons had *p*-values of 0.0156.

Sulfate levels were found to be significantly higher in the roadway runoff than in stream samples as indicated by a Kruskal-Wallis test comparing sampling sites (*p*-value<0.0001). Median values for RO1, RO2 were SC1, 6.95 and 9.94 mg/L, respectively. Overall sulfate levels and variation in the stream were found to be near identical at the upstream site and downstream site with median values for SC1 and SC2 reaching only 3.72, and 3.74 mg/L, respectively.

Total coliform concentrations were highest overall at SC1 followed by RO2 with median values reaching 200,500 and 180,000 CFU/100 mL, respectively. Interestingly, despite this high concentration both with and without the influence of the interstate right-of-way, the median total coliform concentration downstream at site SC2 was nearly six times less than SC1, reaching 34,000 CFU/100 mL. The SC1-SC2 comparison is significant (*p*-value=0.0313) as indicated by a matched pair, Wilcoxon signed rank test. Fecal coliform concentration by site were lowest at the roadway site, RO1 followed by SC2. Concentrations at RO2 and SC1 were among the highest. These findings suggest that fecal contamination from major urban roadways and their right-of-way, may not be a significant source of stream coliform pollution.

Objective B: Relationship of rainfall and flow characteristics on water quality at each site

Storm Type Cluster Analysis

Each storm event sampled at the four sampling sites were clustered and grouped by total precipitation and maximum rain intensity into four separate categories. With each category in place, a nonparametric Kruskal-Wallis test and Wilcoxon rank sum test was used to compare the water quality from one storm type to another at each site. While the Kruskal-Wallis test did not report any significant changes for any pollutant at any site, results of the Wilcoxon rank sum test indicated that site RO2 witnessed a significant difference in water quality for concentrations of TSS, VSS, and $\text{NO}_{2+3}\text{-N}$ (p -values=0.0051, 0.0446, 0.0252, respectively). For these pollutants, the test indicated that ST-3 storms (low total precipitation, moderate maximum rain intensity) yielded significantly higher concentrations compared to ST-1 storms (moderate total precipitation, low maximum rain intensity).

Seasonal Analysis

Results of a nonparametric Kruskal-Wallis test and Wilcoxon rank sum test revealed that unlike storm type categories, seasonal changes had the most influential effect overall on the water quality concentration, especially for the rainfall runoff originating from the roadway at catchments RO1 and RO2. No seasonal change for any pollutant concentration was reported at site SC2.

Solids

Figure 3.4 illustrates significantly elevated spring TSS (a) and VSS (b) concentrations at site RO1 compared to summer as indicated by a Wilcoxon rank sum test (p -values=0.0409 and 0.0152, respectively). Similarly, TSS and VSS concentrations during spring storms at RO1 compared to those occurring in fall were also strongly elevated though not strictly significantly

different (both p -values=0.0553). Spring TSS and VSS concentrations at RO2 were also significantly higher compared to fall events as indicated by a Wilcoxon rank sum test (p -values=0.0177 and 0.0204, respectively). No significant seasonal changes in solids concentrations occurred in either stream site.

Pathogens

No significant seasonal changes in total coliform concentrations occurred over the course of the sampling period at any site, indicated in **Figure 3.5**. Results of a Wilcoxon rank sum test comparing spring and fall fecal coliform EMCs at site RO1 indicated that fall coliform counts were significantly higher than counts occurring in the spring (p -value=0.0062) (**Figure 3.5-b**).

Nutrients

Seasonal variation for nitrite plus nitrate as nitrogen ($\text{NO}_{2+3}\text{-N}$), sulfate (SO_4), and ortho-phosphate (O-PO_4) is summarized in **Figure 3.6-a** through **Figure 3.6-c**. Nitrogen EMCs (**Figure 3.6-a**) occurring in spring at sites RO1 and RO2 were significantly higher than fall levels per a Wilcoxon rank sum test comparing each season to one another (p -values=0.0082 and 0.0338). At site RO1 the spring levels were also significantly higher than summer levels (p -value=0.0268). The upstream site, SC1 had overall higher $\text{NO}_{2+3}\text{-N}$ concentrations during spring, however the seasonal changes was not significantly different compared to summer or fall concentrations due to some very low nitrogen EMCs in addition to high EMCs. A Wilcoxon rank sum test did indicate that fall concentrations were significantly lower than summer levels at site SC1 (p -value=0.0304).

Sulfate EMCs (**Figure 3.6-b**) at RO1 and SC1 were all significantly increased during spring events compared to fall events (p -values=0.0082 and 0.0304, respectively). At RO1 this increase was more than both summer and fall events. At RO2 and again for RO1, spring sulfate

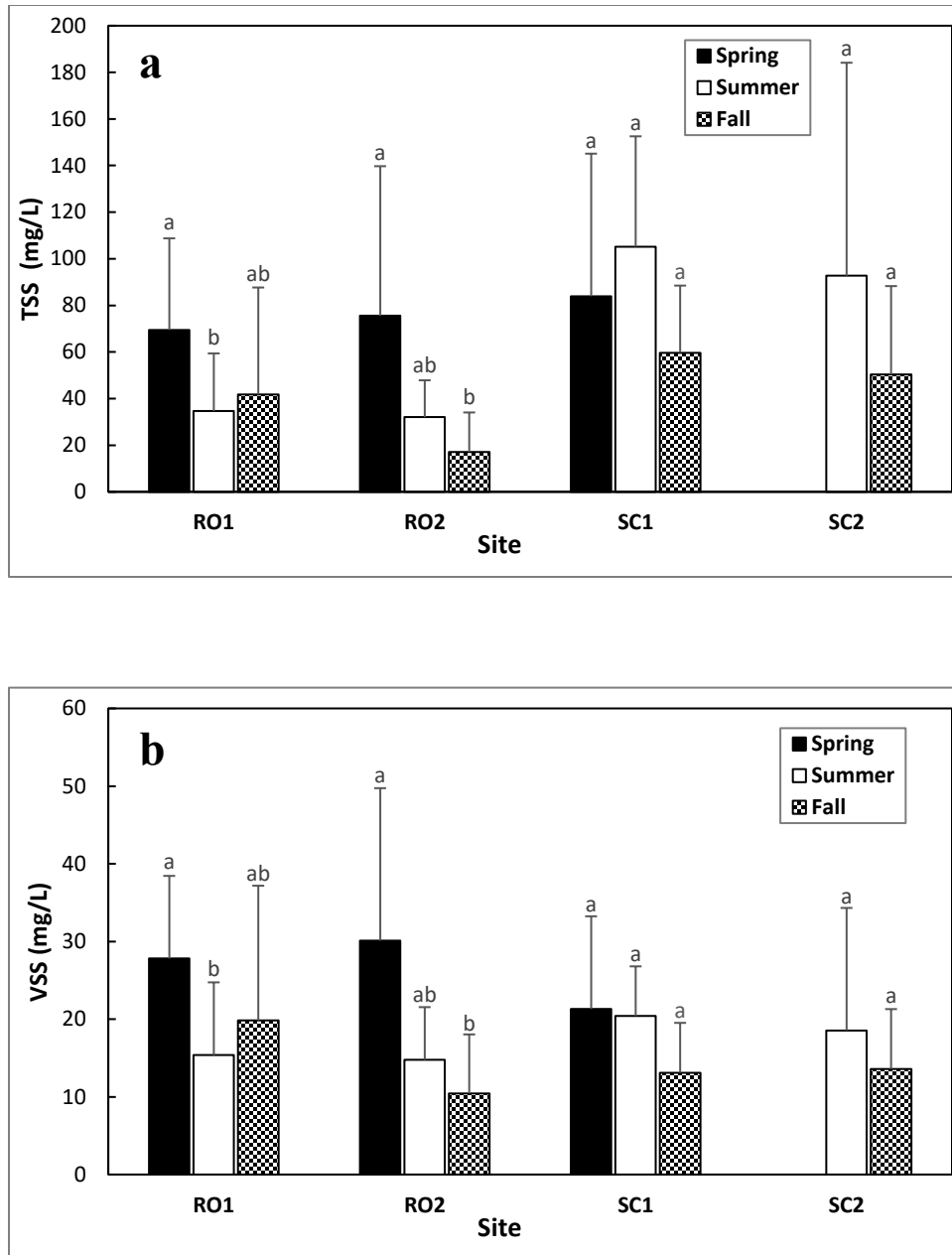


Figure 3.4. Significant differences among TSS (a) and VSS (b) concentrations among each sampling site by season. Spring sampling did not occur at site SC2. Within a site, seasons that share similar lower case letters are not significantly different from one another at a 0.05 level according to the Wilcoxon rank sum test. Throughout this table, the largest means are always denoted by “a” and get smaller with each consecutive letter. Error bars represent standard deviation.

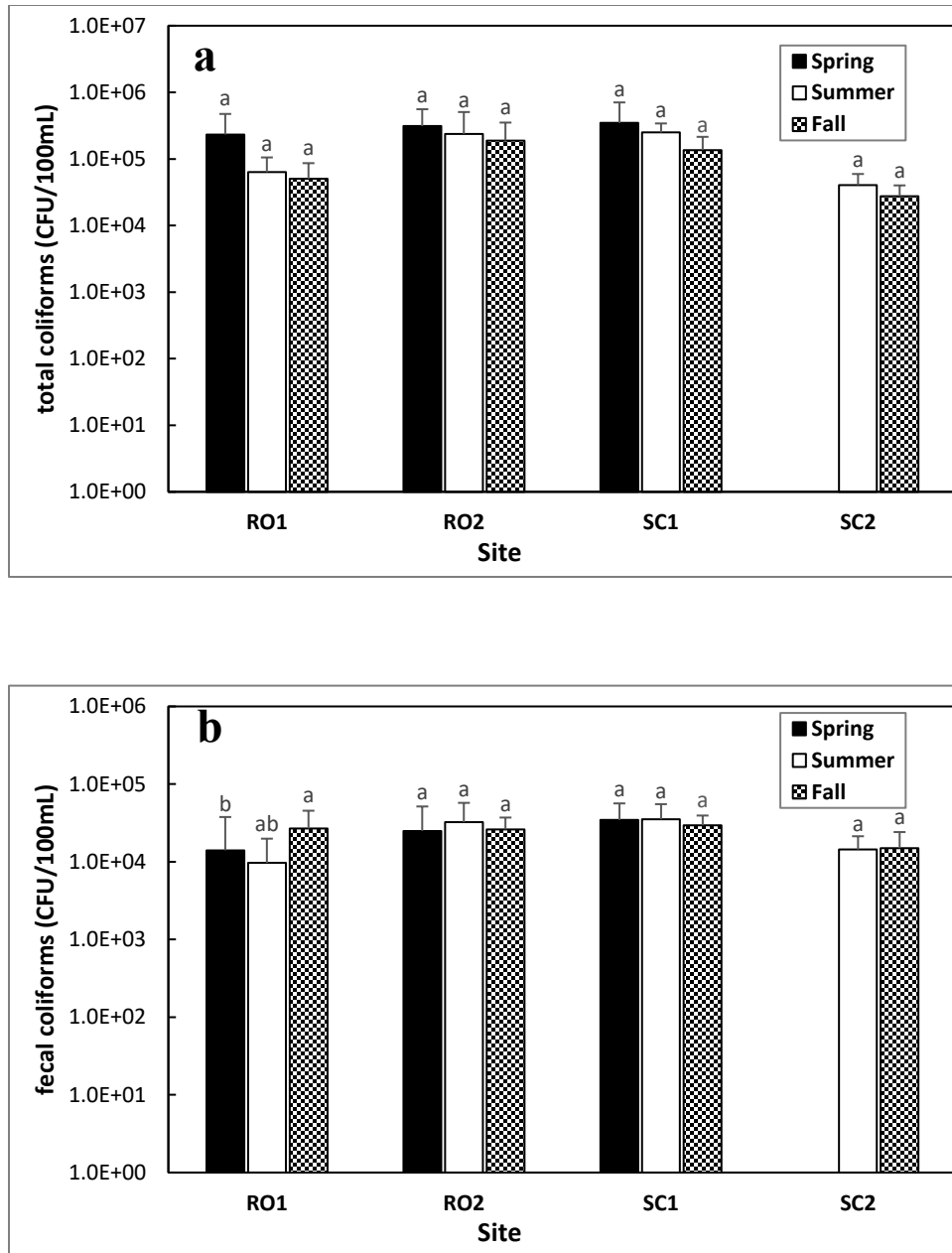


Figure 3.5. Significant differences among Total Coliform (a) and Fecal Coliform (b) concentrations among each sampling site by season. Spring sampling did not occur at site SC2. Within a site, seasons that share similar lower case letters are not significantly different from one another at a 0.05 level according to the Wilcoxon rank sum test. Throughout this table, the largest means are always denoted by “a” and get smaller with each consecutive letter. Error bars represent standard deviation.

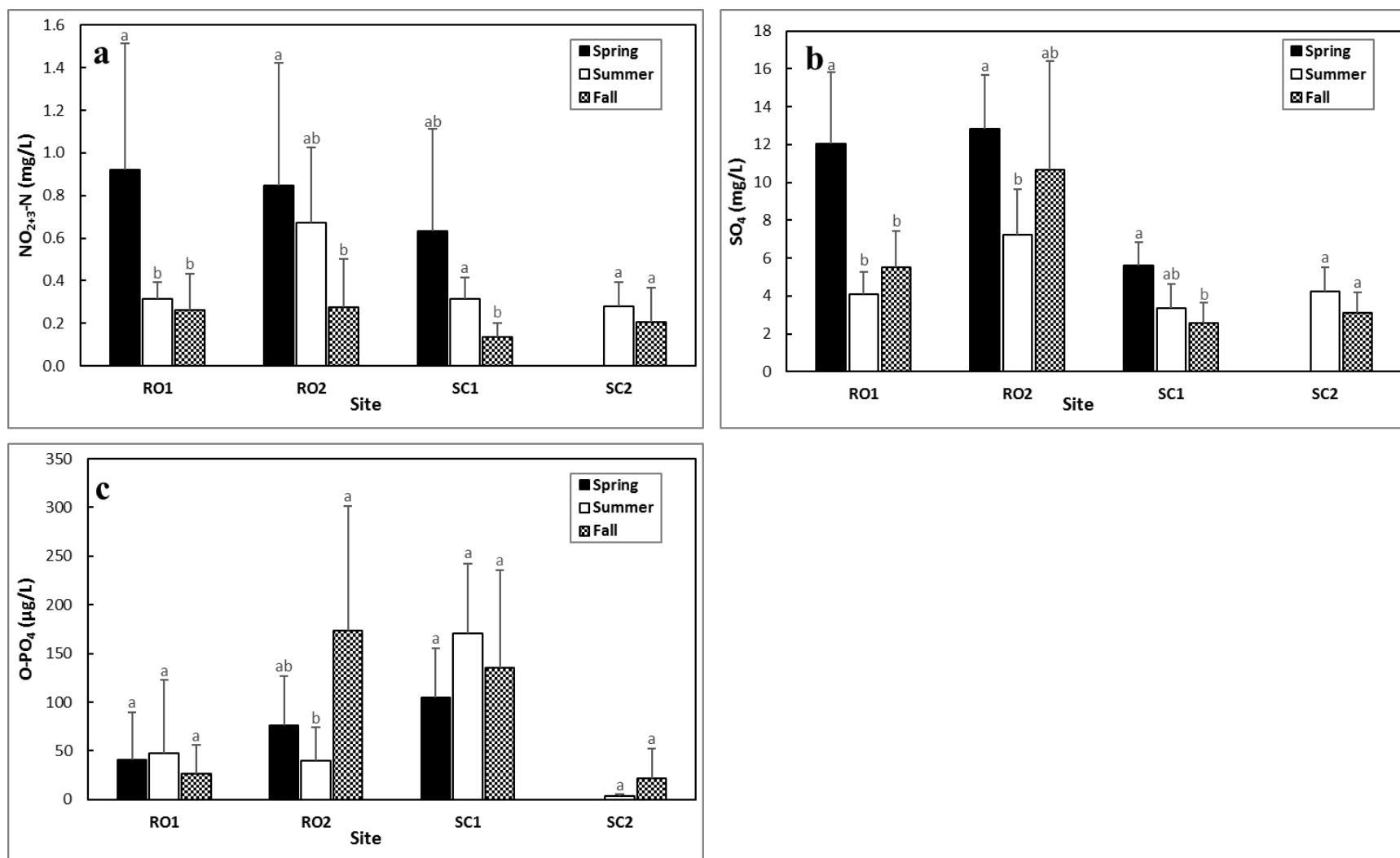


Figure 3.6. Significant differences among $\text{NO}_{2+3}\text{-N}$ (a), SO_4 (b), and O-PO_4 (c) concentrations among each sampling site by season. Spring sampling did not occur at site SC2. Within a site, seasons that share similar lower case letters are not significantly different from one another at a 0.05 level according to the Wilcoxon rank sum test. Throughout this table, the largest means are always denoted by “a” and get smaller with each consecutive letter. Error bars represent standard deviation.

EMCS were significantly increased compared to summer EMCs (p -values=0.0032 and 0.0124, respectively).

As indicated in **Figure 3.6-c**, fall ortho-phosphate concentrations at site RO2 were significantly higher than in summer (p -value=0.0228). There is a rain event that occurred on October 29 that produced a spike in ortho-phosphate at RO2, however it was found that this event does not fully explain this unique seasonal trend in RO2's overall ortho-phosphate concentration. The October 29th storm is unique in that it is the only rainfall event captured at this site where the grass within the catchment area was mowed shortly before the rain event occurred and sampling initiated. The Wilcoxon rank sum test was repeated with the October 29th event excluded from the analysis. Despite the repeated test, fall ortho-phosphate levels were still significantly higher than those produced in the spring (p -value=0.0467). These findings indicate that while cutting grass within a catchment shortly before capturing a rain event may increase the EMCs of some pollutant data, it does not fully explain this seasonal trend at RO2.

Correlation Analysis

For each monitored event, water quality EMCs at each site were correlated to other site specific pollutants monitored throughout the study. Water quality EMCs at each site were also correlated to other explanatory variables described in **Table 3.4**. Correlations were determined using nonparametric Spearman's rank correlation coefficients that also produce p -values so the statistical significance of correlations could be observed. Results of this analysis are summarized in **Tables 3.5** and **3.6**. For simplicity, each table is reduced to show only the sites and explanatory variables where a significant correlation has been found. Correlations not found to be significant are removed.

Table 3.4. Explanatory variables utilized in correlation analyses.

Antecedent climate variable	
ADP	Antecedent dry weather period [days]
Rainfall variables	
P_t	Total precipitation [in]
D_r	Rainfall duration of an event [hr]
I_{ave}	Average rainfall intensity [in/hr]
I_{max5}	Maximum 5-minute rainfall intensity [in/hr]
Stormwater flow variables	
V	Total runoff volume [m ³]
D_v	Runoff duration of an event [hour]
Q_{ave}	Mean flow rate [m ³ /s]
Q_{max5}	Maximum 5-minute flow rate [m ³ /s]
U_{ave}	Average velocity [m/s]
U_{max5}	Maximum 5-minute velocity [m/s]

Correlations among pollutants, shown in **Table 3.5**, show that TSS concentrations do correlate well with VSS at each site, but do not correlate well with any other pollutants variables, except at the downstream sampling point, SC2 where both TSS and VSS solids correlate with indicator organisms. VSS concentrations at the two roadway runoff sites, RO1 and RO2 have significant correlations with NO₂₊₃-N. Nitrogen EMCs at most sites (excluding RO2) were also positively correlated with sulfate levels monitored throughout the study. Interestingly,

nitrogen, as well as sulfate, levels occurring at RO1 had a positively correlated with total coliforms; while at site SC2, the correlation was inversed. These finding indicate the difficulty in modeling pollutant transport at varying locations. Four sampling sites within close proximity to one another in one subwatershed produce distinctly different pollutant transport patterns.

Table 3.6 summarizes significant correlations of site EMCs to various hydrologic and antecedent climate variables. In the case of antecedent dry period, no significant correlation was

Table 3.5. Spearman rank correlation coefficients between water quality concentrations.

Pollutant	pH	TSS				VSS		NO ₂₊₃ -N			O-PO ₄	SO ₄		Total coliform
	RO2	RO1	RO2	SC1	SC2	RO1	RO2	RO1	SC1	SC2	SC1	RO1	SC2	RO2
VSS		<u>0.96</u>	<u>0.97</u>	<u>0.96</u>	<u>0.91</u>	–	–	–	–	–	–	–	–	–
NO ₂₊₃ -N						<u>0.63</u>	<u>0.66</u>	–	–	–	–	–	–	–
SO ₄						0.50		<u>0.75</u>	<u>0.73</u>	<u>0.89</u>	-0.59	–	–	–
Total coliform	-0.63				0.67			<u>0.73</u>				0.60		–
Fecal coliform					0.58					-0.69			-0.77	0.56

Note: All values presented are significant at $p < 0.05$. Bold values are significant at $p < 0.01$. Bold and underlined values are significant at $p < 0.005$. Bold, underlined, and italicized values are significant at $p < 0.0001$.

Table 3.6. Spearman's rank correlation coefficients between water quality concentrations and explanatory variables.

Variable	pH	TSS		VSS		NO ₂₊₃ -N				O-PO ₄		SO ₄			Fecal coliform	
	SC2	RO2	SC2	RO2	SC2	RO1	RO2	SC1	SC2	RO2	SC1	RO1	RO2	SC1	RO1	SC2
ADP																<u>0.72</u>
P_t		-0.46					-0.49	-0.67								
D_r		-0.46	0.53				-0.45							-0.69		0.67
I_{ave}			0.58		0.63		0.46	<u>0.75</u>					-0.46			
I_{max5}			<u>0.69</u>		<u>0.66</u>											
V		-0.53		-0.51												
D_v		<u>-0.68</u>		<u>-0.65</u>		-0.49	-0.51		-0.56		0.62	-0.47		<u>-0.80</u>		
Q_{ave}	-0.56		0.51							0.46	0.73	-0.53		-0.64		
Q_{max5}			<u>0.70</u>		0.52					0.53	0.71			<u>-0.76</u>		
U_{ave}	-0.52		0.55													
U_{max5}			<u>0.71</u>		0.56					-0.45				-0.60		

Note: All values presented are significant at $p < 0.05$. Bold values are significant at $p < 0.01$. Bold and underlined values are significant at $p < 0.005$.

detected except for fecal coliform concentrations at site RO1. Here, fecal coliforms significantly increase with ADP length, indicating a possible incubation effect occurring either on the roadway surface or within the conveyance pipe.

The influence of rainfall and flow-based explanatory variables is mixed throughout the watershed. Suspended solids stemming from roadway runoff was inversely correlated with the total precipitation, total volume, and duration. Conversely, SC2's suspended solids EMCs all correlated positively to their explanatory variables and responded more to rain intensity, flow rate, and velocity. The opposite is true for suspended solids samples taken downstream, at site SC2. Significant nutrient correlations seemed to follow more universal transport mechanisms. Nitrogen, ortho-phosphate, and sulfate EMCs all followed similar trends of positive or inverse correlation regardless of site.

Objective C: Determination of relative contribution of pollutant loading from the roadway

A collection of 26 storm events were monitored and sampled at the study site. Due to instrument failures and the delay in the installation of the SC2 sampling station (prolonged approval process by local city officials), only a subset of the storm events produced data suitable for pairwise analysis of relative contribution of pollutant loading. Distribution free Kruskal-Wallis tests and Wilcoxon rank sum tests were used to determine any significant differences in loading among different storm types. Geometric mean was used to represent the average loading contribution due to the log-normal distribution of the dataset.

Contribution of TSS from interstate roadway runoff (Road)

Pairwise TSS loading results were available for both the interstate (pavement runoff) and SC2 during 14 storm events in total (**Table 3.7**). Large variations were observed in the TSS

Table 3.7. TSS loading and relative contribution from interstate roadway stormwater runoff (Road) to receiving stream (SC2).

Date	Storm Type	Loading (kg/event)		Percent Contribution (RO1/SC2)
		Interstate (Road)	Receiving Stream (SC2)	
7/18/2014	ST-1	15.3	66.3	23.1%
7/20/2014	ST-2	7.23	31.5	23.0%
7/27/2014	ST-4	51.8	1,502	3.4%
8/2/2014	ST-4	52.3	986	5.3%
8/10/2014	ST-2	14.4	112	12.8%
8/20/2014	ST-3	3.86	110	3.5%
8/30/2014	ST-1	57.6	371	15.6%
9/2/2014	ST-2	12.8	77.6	16.5%
9/11/2014	ST-3	83.7	346	24.2%
10/6/2014	ST-3	70.2	55.5	* 126.5%
10/10/2014	ST-2	16.4	485	3.4%
10/14/2014	ST-1	33.5	445	7.5%
10/29/2014	ST-2	21.3	25.5	83.4%
11/17/2014	ST-1	33.5	958	3.5%
Geometric Mean				10.6%

* Outliers removed from the calculation of the mean relative contribution (SC1/SC2)

loading from roadway runoff, with a factor of 25 between the smallest and greatest data points. Even larger variations were present in the TSS loading observed in the receiving stream, which varied by a factor of 48. It is noted that during the storm event occurring on 10/6/2014, the relative contribution of TSS from the roadway to the receiving stream was unusually large, exceeding 100%. It is not clear what factors were attributable to this anomaly. To represent the more common storm conditions at the study site, this outlier was removed from the calculation of the mean relative contribution of TSS in roadway runoff from the interstate to the receiving stream. The contribution of TSS from interstate pavement in the subwatershed averaged 10.6%, indicating that the roadway is not likely the major contributor of TSS to the receiving stream in the subwatershed of this study. The results of the Kruskal-Wallis test did not indicate a

significant change overall in relative loading (p -value=0.5566) from one storm type to another despite the varying contribution from each storm event.

Contribution of TSS from upstream (SC1)

Frequent sensor malfunctions of the ISCO 750 area velocity module at SC1 lead to fewer sampled storm events needed for comparison. TSS loading results were available for both the SC1 (stream flow upstream of the roadway stormwater runoff entry points) and SC2 (stream flow downstream of the roadway stormwater runoff entry points) during 9 storm events only (Table 3.8). During the storm on 8/20/2014, the TSS loading in the upstream stream flow exceeded the downstream stream flow (**Table 3.8**). Thus, this data point was removed as an outlier during further data analysis. The upstream loading contribution was less varied compared to that from the interstate, and ranged from 3.6% to 54.0%. Kruskal-Wallis testing indicated no significant influence of the four storm types on the loading variance (p -value=0.4653). The mean relative contribution of TSS carried from the upstream portion of the watershed (SC1) to the downstream portion (SC2) was 13.6%. While this was slightly greater than the contribution from the pavement runoff (Road), neither the roadway runoff nor the upstream flow appeared to be the primary sources of TSS to the receiving stream (SC2). Therefore, other uncharacterized sources in the subwatershed were contributing most TSS loading to the receiving stream.

Contribution of fecal indicator from roadway runoff (Road)

Using fecal coliform (FC) as the microbiological indicator, we determined the loading of potential pathogen indicators in the stormwater runoff from the roadways. Of the eleven storm events where FC loading data were available for both pavement runoff (Road) and the receiving stream (SC2), one storm event on 10/29/2014 was considered as an outlier based on the unusually high percentage of FC loading (**Table 3.9**). Excluding the outlier, the mean

Table 3.8. TSS loading and relative contribution from upstream (SC1) to receiving stream (SC2).

Date	Storm Type	Loading (kg/event)		Percent Contribution (SC1/SC2)
		Upstream (SC1)	Receiving Stream (SC2)	
8/2/2014	ST-4	533	986	54.0%
8/10/2014	ST-2	30.0	112	26.7%
8/20/2014	ST-3	111	110	*100.6%
8/30/2014	ST-1	69.1	371	18.6%
9/2/2014	ST-2	10.8	77.6	13.9%
9/11/2014	ST-3	20.9	346	6.1%
10/10/2014	ST-2	17.5	485	3.6%
10/14/2014	ST-1	119	445	26.7%
11/17/2014	ST-1	51.0	958	5.3%
Geometric Mean				13.6%

* Outliers removed from the calculation of the mean relative contribution (SC1/SC2)

Table 3.9. Fecal coliform loading and relative contribution from interstate roadway stormwater runoff (Road) to the receiving stream (SC2).

Date	Storm Type	Loading (CFU×10 ¹⁰ /event)		Percent Contribution (Road/SC2)
		Interstate (Road)	Receiving Stream (SC2)	
7/18/2014	ST-1	37.4	59.7	62.6%
7/20/2014	ST-2	2.78	10.5	26.4%
8/2/2014	ST-4	9.29	125	7.4%
8/10/2014	ST-2	1.02	29.0	3.5%
8/20/2014	ST-3	1.85	25.7	7.2%
8/30/2014	ST-1	29.4	76.0	38.7%
9/2/2014	ST-2	11.6	84.9	13.7%
9/11/2014	ST-3	46.4	71.6	64.9%
10/6/2014	ST-3	8.53	10.8	78.7%
10/10/2014	ST-2	8.00	126	6.3%
10/29/2014	ST-2	58.2	22.9	*253.5%
Geometric Mean				18.7%

* Outliers removed from the calculation of the mean relative contribution (SC1/SC2)

contribution of FC loading from the interstate pavement (Road) accounted for 18.7% of the FC loading in the receiving stream (SC2), indicating that the roadway was also not a major source of microbiological contamination in the watershed. Utilizing the Kruskal-Wallis test, the varying loading percentages for each event were compared based on storm type. The results of the test indicated that storm type did not have a significant influence in relative loading.

Contribution of fecal indicator from upstream (SC1)

Due to frequent sensor malfunctions of the ISCO 750 area velocity module at SC1, only six storm events had FC loading data for both the SC1 (stream flow upstream of the roadway stormwater runoff entry points) and SC2 (stream flow downstream of the roadway stormwater runoff entry points) (**Table 3.10**). The mean of relative contribution transported from upstream (SC1) was 20.6%, ranging from the low of 2.7% to the high of 46.6%. Storm type comparison did not reveal a significant influence on the varying loading as per the results of a Kruskal-Wallis test. Similar to TSS loading distribution, the upstream flow transported slightly greater amount of fecal coliform to the downstream flow than the interstate pavement did. These results show that other sources contributed the majority of FC loading to the receiving stream.

Table 3.10. Fecal coliform loading and relative contribution from upstream (SC1) to the receiving stream (SC2).

Date	Storm Type	Loading (CFU×10 ¹⁰ /event)		Percent Contribution (SC1/SC2)
		Upstream (SC1)	Receiving Stream (SC2)	
8/10/2014	ST-2	12.2	29.0	42.3%
8/20/2014	ST-3	12.0	25.7	46.6%
8/30/2014	ST-1	33.3	76.0	43.9%
9/2/2014	ST-2	2.26	84.9	2.7%
9/11/2014	ST-3	11.6	71.6	16.3%
10/10/2014	ST-2	25.5	126	20.3%
Geometric Mean				20.6%

Contribution of nitrogen from roadway runoff (Road)

The nitrogen loading results were available for both the interstate (pavement runoff) and SC2 (downstream point of the receiving stream) during 11 storm events in the study period (**Table 3.11**). The contribution stemming from the roadway ranged from a low of 6.6% up to 64.8%. No outliers were present in the data. The geometric mean relative contribution of these 11 storm events was 22.8%. A Kruskal-Wallis test indicated no overall significant change in loading from one storm type to another (p -value=0.1029), however a Wilcoxon rank sum test did indicate that type 2 storms (low precipitation, low maximum intensity) resulted in significantly lower relative loading than type 1 storms (moderate precipitation, low maximum intensity) (p -value=0.0373). These findings suggest that more $\text{NO}_{2+3}\text{-N}$ enters the receiving stream during steady, longer duration storms than events characterized by a short burst of rainfall.

Table 3.11. $\text{NO}_{2+3}\text{-N}$ loading and relative contribution from interstate roadway stormwater runoff (Road) to the receiving stream (SC2).

Date	Storm Type	Loading (kg/event)		Percent Contribution (Road/SC2)
		Interstate (Road)	Receiving Stream (SC2)	
7/18/2014	ST-1	0.343	0.529	64.8%
7/20/2014	ST-2	0.146	0.706	20.7%
7/27/2014	ST-4	0.323	2.28	14.2%
8/10/2014	ST-2	0.115	1.09	10.5%
8/20/2014	ST-3	0.099	0.571	17.3%
8/30/2014	ST-1	0.274	0.528	51.9%
9/2/2014	ST-2	0.131	0.663	19.7%
10/10/2014	ST-2	0.064	0.966	6.6%
10/14/2014	ST-1	0.411	1.68	24.5%
10/29/2014	ST-2	0.521	1.85	28.2%
11/17/2014	ST-1	0.700	1.30	53.7%
Geometric Mean				22.8%

Contribution of nitrogen from upstream (SC1)

Six events out of seven were captured to measure the nitrogen loading results for both the SC1 (stream flow upstream of the roadway stormwater runoff entry points) and SC2 (stream flow downstream of the roadway stormwater runoff entry points) (**Table 3.12**). One event on 8/02/2014 was deemed an outlier and not included in the analysis since the relative loading measured over 100%. The geometric mean of these six events was measured as 11.6% relative nitrogen contribution to the downstream waterway. This indicates that the nitrogen loading upstream of the roadway is not likely the major contributor to the receiving stream in the subwatershed of this study. The Kruskal-Wallis test did not indicate any significant changes based on storm type (p-value=0.1173) for the six events sampled. Increasing the number of events for pairwise comparison may lead to more definitive results as to whether storm type has an influence on the results.

Table 3.12. NO₂₊₃-N loading and relative contribution from upstream (SC1) to the receiving stream (SC2).

Date	Storm Type	Loading (kg/event)		Percent Contribution (SC1/SC2)
		Upstream (SC1)	Receiving Stream (SC2)	
8/2/2014	ST-4	0.832	0.764	*108.9%
8/20/2014	ST-3	0.328	0.571	57.4%
8/30/2014	ST-1	0.117	0.528	22.2%
9/2/2014	ST-2	0.022	0.663	3.3%
10/10/2014	ST-2	0.043	0.966	4.4%
10/14/2014	ST-1	0.414	1.68	24.7%
11/17/2014	ST-1	0.070	1.30	5.4%
Geometric Mean				11.6%

* Outliers removed from the calculation of the mean relative contribution (SC1/SC2)

Part 4: Discussion

Relative Contribution

It was assumed that the roadway stormwater runoff (RO1) could be a major source of pollutant loading to the receiving streams. Other studies have noted how highways are noted as a significant source of non-point pollution (Opher and Friedler 2010, Barrett et al. 1995, Lord 1987, Brezonik and Stadelmann 2002, Buffleben et al. 2002). The mass-based analysis performed in this study shows that roadway stormwater runoff represented a varied, yet overall nonsignificant contributor overall in the subwatershed, accounting for 8.9% of the TSS loading and 16.0% of the FC loading, respectively (**Figure 4.1** and **Figure 4.2**) However, at 22.8% the nitrogen loading from the roadway (**Figure 4.3**) may be more a significant source. While the roadway's contribution of nitrogen to the receiving stream does not represent the majority, it does indicate a possible point of interest of remediation to reduce the concentration of nitrogen in the stream.

Another source of pollutant contribution was the upstream flow, which accounted for 13.6%, 20.6%, and 11.6% of the pollutant loading in the downstream flow, for TSS, FC, and $\text{NO}_{2+3}\text{-N}$, respectively (**Figure 4.1** through **Figure 4.3**) These two known sources (RO1 and SC1) together contributed 22.5% of the TSS loading, 36.6% of the FC loading, and 34.4% of the nitrogen loading in the receiving stream (SC2). Thus, a large majority of the pollutant loading, i.e. 77.5% of the TSS loading, 63.5% of the FC loading, and 65.6% entered the receiving stream from sources other than the roadway and upstream flow. Since the study site was situated in a highly-commercialized area, it is likely that local traffic and surrounding businesses could contribute significant pollutant loading to the receiving stream.

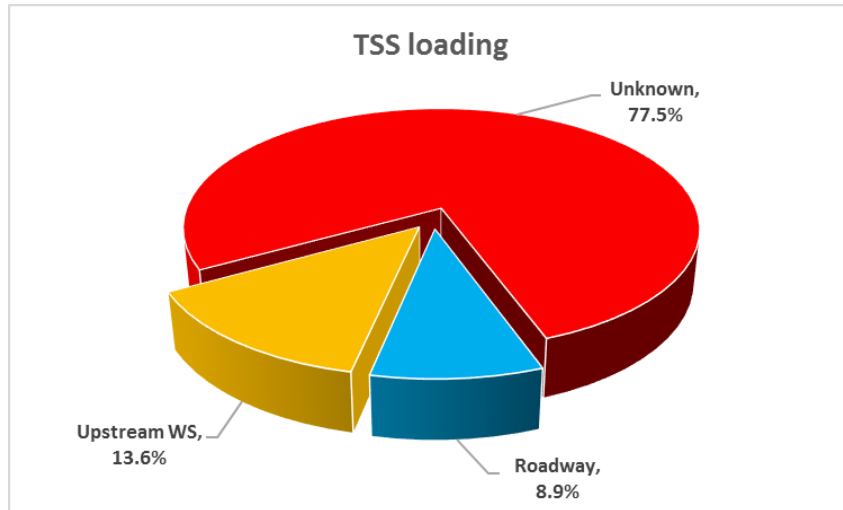


Figure 4.1. Distribution of TSS loading to the receiving stream (SC2).

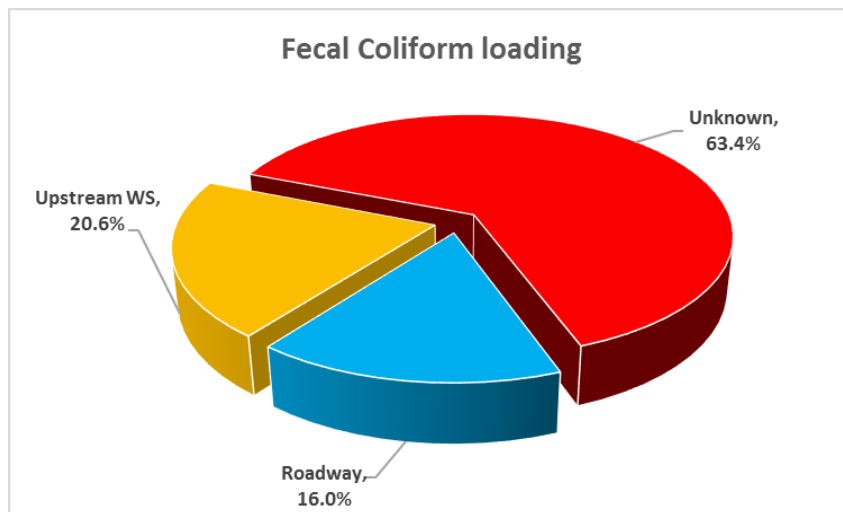


Figure 4.2. Distribution of fecal coliform loading to the receiving stream (SC2).

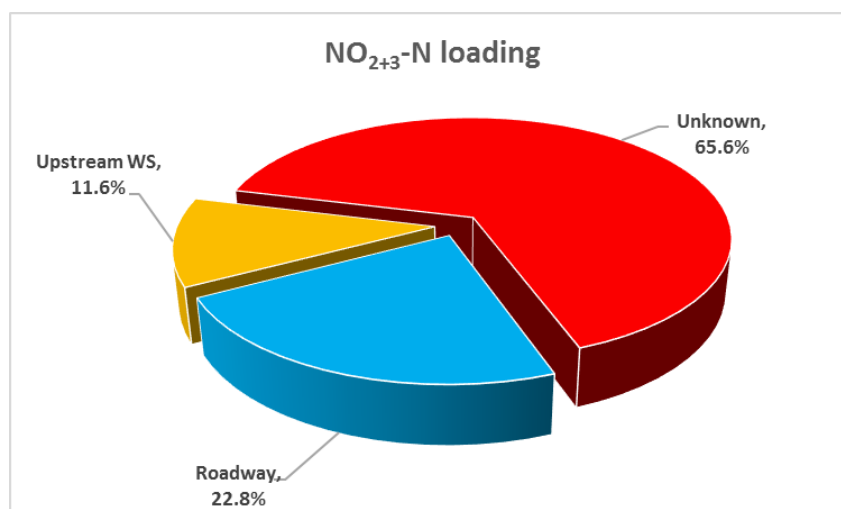


Figure 4.3. Distribution of Nitrite plus nitrate loading to the receiving stream (SC2).

It should be noted that the monitoring site (SC2) for the receiving stream (downstream of RO1 and SC1) was quite distant (~1 km) from the other monitoring sites, with an area of wetland lying in between the study site and the SC2 monitoring site. It is possible that the wetland could have served as a mitigating function, reducing the pollutant loading reaching the downstream SC2. Thus, the relative contribution from the roadways shown in this study could be overestimated and the actual contribution might be even lower.

Impact of location

For this study, it was expected that total and fecal coliforms concentrations would not be higher in the upstream watershed than the downstream watershed. While this finding may provide evidence that highway sources of indicator organisms may not have much impact on the water quality of the receiving stream, other explanations are possible. Perhaps the location of the sampling sites was not ideal and that land use factored in more variables than expected. Site SC2 was approximately 1-km downstream of site SC1, which may be too far away to make reasonable comparisons of the water quality upstream. It also may be possible that another

source of coliforms near the upstream sampling site led to an inflated coliform count. Driscoll et al. (1990) reported that surrounding land use is the most important general factor influencing pollutant loads in highway runoff.

Part 5: Conclusion

A total of 26 rainfall events were sampled among the four sites between March, 2014 and November, 2014. Rainfall events were varied but were categorized into four “storm type” categories. Distribution free Kruskal-Wallis and Wilcoxon signed rank tests were performed on water quality EMCs in two ways, seasonal changes and storm type. The results indicated that while storm type had no significant influence on water quality at each site, seasonal analysis revealed increased nutrient and suspended solid concentrations during spring events.

Correlation analysis showed numerous significant relationships, though not all sites shared the same correlations. Antecedent dry period seems to have a strong influence on fecal coliform EMCs at site RO1. It is possible that routinely flushing out the conveyance pipe underneath the roadway may serve a mitigating effect on indicator organisms at site RO1. Many of the relationships between pollutants were not logical and were likely coincidental in fashion. Further study is needed understand the transport mechanisms that lead to the correlation results at each site.

Results from the relative loading contribution study indicated two things: 1.) sediment and fecal indicator microorganisms indicate that upstream flow as well as road surface runoff remained a minor contributor to downstream pollutant loading, and 2.) Large temporal variations existed in the pollutant loading from the roadway stormwater runoff to the receiving stream. However, analysis of the temporal variations based on storm type did not result in a significant difference. More samples may be need to confirm these findings.

References

- APHA, 2005. Standard Methods for the Examination of Water and Wastewater.
- Appel, P.L., and Hudak, P.F., 2001. Automated sampling of stormwater runoff in an urban watershed, North-Central Texas. *Journal of Environmental Science and Health, Part A* 36 (6), 897-907.
- Barrett, M.E., Zuber, R.D., Collins, E.R., III, Malina, J.F., Jr., Charbeneau, R.J., and Ward, G.H. 1995. A review and evaluation of literature pertaining to the quantity and control of pollution from highway runoff and construction, 2nd Ed. Technical Report. 239, Center for Research in Water Resources, The University of Texas at Austin.
- Brezonik, P.L., and Stadelmann, T.H., 2002. Analysis and predictive models of stormwater runoff volumes, loads, and pollutant concentrations from watersheds in the Twin Cities metropolitan area, Minnesota, USA." *Water Research*, 36 (7), 1743-757.
- Buffleben, M.S., Zayeed, K., Kimbrough, D., Stenstrom, M.K., and Suffet, I.H., 2002. Evaluation of urban non-point source runoff of hazardous metals entering Santa Monica Bay, California. *Water Science and Technology*, 45 (9), p.263-268.
- Driscoll, E.D., Shelley, P.E., and Strecker, E., 1990. Pollutant loadings and impacts from highway stormwater runoff Volume III: Analytical investigation and research report. Rep. No. FHWA-RD-88-008, Fed. Hwy. Administration, Ofc. of Res. and Devel., Washington, D.C.
- EPA, U.S., 2009. National water quality inventory: report to Congress, Tech. rep., Washington, DC: Environmental Protection Agency.
- FHWA, 2001. Guidance manual for monitoring highway runoff water quality, (June), p.200.
- Gupta, M. K., Agnew, R. W., Gruber, D., and Kreutzberger, W., 1981. Constituents of highway runoff. Volume IV: Characteristics of runoff from operating highways. Res. Rep. No. FHWD-RD-81-045, Fed. Hwy. Administration, Washington, D.C.
- Helmreich, B. et al., 2010. Runoff pollutants of a highly trafficked urban road - Correlation analysis and seasonal influences. *Chemosphere*, 80(9), pp.991–997.
- Hoffman, E. et al., 1985. Stormwater runoff from highways. *Water, Air, and Soil Pollution*, 25(4), pp.349–364.
- Hollander, M. and Wolfe, D.A., 1999, Nonparametric statistical methods, 2nd edition. John Wiley and Sons Inc., New York, NY.
- Huber, W.C. and Maidment, D.R., 1992. Contaminant transport in surface water. *Handbook of hydrology*, pp.11–14.
- Lee, J., Bang, K., Ketchum, L., Choe, J., and Yu, M., 2002. First flush analysis of urban storm runoff. *Science of The Total Environment*, 293(1), 163-175.

- Lord, B.N., 1987. Nonpoint source pollution from highway stormwater runoff. *Science of The Total Environment*, 59, 437–446.
- Jr., Irish, L.B., Lesso, P.D., Barrett, M.S., and Jr., Malina, J.F., and Charbeneau, R.J., 1995. An evaluation of the factors affecting the quality of highway runoff in the Austin, Texas area. Technical Report. 236, Center for Research in Water Resources, The University of Texas at Austin.
- Mallin, M.A., Johnson, V.L. and Ensign, S.H., 2009. Comparative impacts of stormwater runoff on water quality of an urban, a suburban, and a rural stream. *Environmental Monitoring and Assessment*, 159 (1), 475–491.
- Mitton, B.G.B., and Payne, G.A. 1997. Quantity and quality of runoff from selected guttered and unguttered roadways in northeastern Ramsey County, Minnesota, Technical Report, 67, U.S. Geological Survey.
- Opher, T. & Friedler, E., 2010. Factors affecting highway runoff quality. *Urban Water Journal*, 7 (3), 155–172.
- Sartor, J.D., Boyd, G.B. & Agardy, F.J., 1974. Water pollution of street surface contaminants. *Journal (Water Pollution Control Federation)*, 46 (3), 458–467.
- U.S. Environmental Protection Agency, 2009. National Water Quality Inventory: Report to Congress. EPA 841-R-08-001. United States Environmental Protection Agency, Office of Water, Washington D.C., 43
- U.S. Environmental Protection Agency. 1999. Protocol for Developing Sediment TMDLs. EPA 841-B-99-004. United States Environmental Protection Agency, Office of Water, Washington D.C., 132.
- Zhang, Y. and He, Q. 2013. Characterization of bacterial diversity in drinking water by pyrosequencing. *Water Sci. Technol.-Water Supply* 13 (2), 358-367.
- Zhang, Y., Zamudio Cañas, E.M., Zhu, Z., Linville, J.L., Chen, S., and He, Q., 2011. Robustness of archaeal populations in anaerobic co-digestion of dairy and poultry wastes. *Bioresour. Technol.* 102 (2), 779-785.

Appendices

Appendix A, Chemical and hydrological characteristics at each site

Table A.1. Physical and chemical characteristics of water samples at site RO1.

Date	Volume (m ³)	pH	TSS (mg/L)	VSS (mg/L)	NO ₂₊₃ -N (mg/L)	O-PO ₄ (µg/L)	SO ₄ (mg/L)	Total Coliform (CFU/100 mL)	Fecal Coliform (CFU/100 mL)
3/16/2014	33	7.89	80.0	36.0	0.51	17.1	14.2	—	—
4/27/2014	2.5	7.41	50.7	27.1	1.30	31.2	18.8	727,000	11,000
4/28/2014	140	8.03	89.3	34.3	0.39	22.2	7.82	88,000	4,000
4/30/2014	28	7.56	35.7	22.1	0.51	ND ^a	7.43	3,000	500
5/14/2014	25	7.97	35.0	16.7	0.56	16.2	9.92	275,000	4,000
5/23/2014	16	8.46	141	43.1	1.96	122	12.6	110,000	9,000
5/25/2014	11	7.39	96.3	31.9	1.54	113	14.2	140,000	3,000
7/18/2014	25	6.93	27.5	11.3	0.61	ND	11.5	288,000	67,000
7/20/2014	21	7.16	15.6	5.63	0.32	ND	5.94	50,000	6,000
7/27/2014	35	7.59	68.1	21.3	0.42	ND	3.53	33,000	13,000
8/2/2014	141	7.58	16.9	8.75	—	—	—	130,000	3,000
8/10/2014	15	7.85	42.5	23.8	0.34	ND	4.61	78,000	3,000
8/20/2014	21	7.55	8.33	6.67	0.21	176	3.42	10,000	4,000
8/30/2014	46	7.84	56.9	26.3	0.27	53.3	2.87	78,000	29,000
9/2/2014	31	8.93	18.8	11.3	0.19	ND	5.19	60,000	17,000
9/11/2014	49	7.82	77.5	26.9	0.43	ND	5.20	65,000	43,000
10/6/2014	24	7.98	132	56.7	—	—	—	28,000	16,000
10/10/2014	33	7.96	22.5	11.9	0.09	19.2	8.12	10,000	11,000
10/14/2014	146	8.32	10.4	10.4	0.13	80.3	2.48	—	—
10/29/2014	46	8.03	20.8	13.3	0.51	40.2	6.95	110,000	57,000
11/17/2014	138	7.90	11.0	8.50	0.23	15.1	5.29	30,000	17,000

^aND, not detected.

Table A.2. RO1 rainfall and flow characteristics.

Date	Season	ADP (days)	P_t (in.)	I_{ave} (in/hr)	I_{max5} (in/hr)	Q_{ave} (l/s)	Q_{max5} (l/s)	V (m ³)	D_v (hr)
3/16/2014	Spring	13	0.47	0.06	0.20	0.6	14	33	16
4/27/2014	Spring	5.3	0.06	0.07	0.12	1.2	2.3	2.5	0.6
4/28/2014	Spring	0.9	1.40	0.13	5.52	5.0	151	140	7.9
4/30/2014	Spring	0.8	0.18	0.09	0.36	3.0	10	28	2.6
5/14/2014	Spring	5.1	0.43	0.05	0.36	0.5	6.8	25	14
5/23/2014	Spring	7.7	0.12	1.44	1.44	10	38	16	0.5
5/25/2014	Spring	2.3	0.10	0.25	0.72	5.6	20	11	0.5
7/18/2014	Summer	10	0.45	0.08	0.48	2.8	8.4	25	2.5
7/20/2014	Summer	0.7	0.14	0.13	0.48	4.7	12	21	1.2
7/27/2014	Summer	7.6	1.03	0.61	3.96	8.3	31	35	1.1
8/2/2014	Summer	5.9	1.07	2.29	4.80	84	189	141	0.5
8/10/2014	Summer	2.0	0.23	0.49	0.72	3.6	14	15	1.2
8/20/2014	Summer	0.2	0.31	0.23	1.44	6.1	34	21	1.0
8/30/2014	Summer	10	0.39	0.12	0.60	5.9	36	46	2.2
9/2/2014	Fall	2.9	0.24	0.08	0.60	3.0	10	31	2.9
9/11/2014	Fall	8.6	0.34	0.18	2.04	6.9	33	49	2.0
10/6/2014	Fall	3.1	0.20	0.17	0.96	10	20	24	0.7
10/10/2014	Fall	2.3	0.26	0.05	0.72	2.6	10	33	3.5
10/14/2014	Fall	0.9	0.77	0.20	0.96	14	48	146	3.0
10/29/2014	Fall	13	0.27	0.05	0.24	2.9	11	46	4.4
11/17/2014	Fall	10	0.74	0.09	0.48	2.3	22	138	17

Table A.3. Physical and chemical characteristics of water samples at site RO2.

Date	Volume (m ³)	pH	TSS (mg/L)	VSS (mg/L)	NO ₂₊₃ -N (mg/L)	O-PO ₄ (µg/L)	SO ₄ (mg/L)	Total Coliform (CFU/100 mL)	Fecal Coliform (CFU/100 mL)
3/16/2014	123	8.06	33.0	20.0	0.31	ND ^a	17.9	—	—
3/29/2014	22	7.96	156	55.0	0.23	ND	8.57	—	—
4/27/2014	7.7	7.32	89.2	44.2	1.01	69.3	11.3	725,000	75,000
4/28/2014	309	7.83	47.1	20.0	0.72	121	15.5	408,000	17,000
4/30/2014	71	7.60	17.1	8.57	0.44	84.3	11.2	48,000	7,000
5/14/2014	144	7.95	23.1	11.9	0.69	76.3	13.9	190,000	7,000
5/23/2014	21	8.38	189	58.8	1.81	142	11.6	123,000	34,000
5/25/2014	23	7.24	50.6	22.5	1.56	108	12.7	370,000	10,000
6/4/2014	27	7.85	37.0	13.4	0.68	30.2	5.41	23,000	7,000
6/5/2014	32	7.28	49.4	20.0	0.72	24.2	9.09	755,000	67,000
6/25/2014	32	7.74	45.6	20.6	1.04	54.3	5.54	203,000	14,000
6/29/2014	26	8.14	40.0	19.4	1.18	87.3	8.11	135,000	35,000
7/18/2014	69	6.79	22.5	10.6	0.57	ND	10.7	430,000	51,000
7/20/2014	43	7.52	3.75	1.88	0.23	ND	8.08	10,000	2,000
8/30/2014	117	7.96	26.3	17.5	0.29	79.3	3.84	105,000	50,000
9/2/2014	78	7.51	12.5	9.38	0.29	44.2	9.17	193,000	44,000
9/11/2014	136	7.07	33.1	11.9	—	—	—	457,000	29,000
10/6/2014	49	8.29	48.3	26.7	—	—	—	38,000	22,000
10/10/2014	100	8.08	5.00	5.00	0.06	116	15.2	85,000	18,000
10/14/2014	418	7.96	4.38	4.38	0.15	155	5.20	—	—
10/29/2014	167	8.05	8.33	8.33	0.65	385	18.1	—	—
11/17/2014	451	7.95	8.50	9.50	0.23	165	5.72	170,000	18,000

^aND, not detected.

Table A.4. RO2 rainfall and flow characteristics.

Date	Season	ADP (days)	P_t (in.)	I_{ave} (in/hr)	I_{max5} (in/hr)	Q_{ave} (l/s)	Q_{max5} (l/s)	V (m ³)	D_v (hr)
3/16/2014	Spring	13	0.47	0.06	0.20	1.7	9.3	123	20
3/29/2014	Spring	11	0.19	0.05	0.36	3.6	10	22	1.7
4/27/2014	Spring	5.3	0.06	0.07	0.12	3.2	5.5	7.7	0.7
4/28/2014	Spring	0.9	1.40	0.13	5.52	8.4	140	309	10
4/30/2014	Spring	0.8	0.18	0.09	0.36	6.2	20	71	3.2
5/14/2014	Spring	5.1	0.43	0.05	0.36	2.7	11	144	15
5/23/2014	Spring	7.7	0.12	1.44	1.44	14	38	21	0.4
5/25/2014	Spring	2.3	0.10	0.25	0.72	7.0	24	23	0.9
6/4/2014	Summer	6.1	0.19	0.42	1.56	8.3	44	27	0.9
6/5/2014	Summer	0.7	0.20	0.16	1.20	2.2	55	32	4.1
6/25/2014	Summer	3.4	0.20	0.14	0.84	11	30	32	0.8
6/29/2014	Summer	2.8	0.15	0.15	0.60	7.5	17	26	1.0
7/18/2014	Summer	10	0.45	0.08	0.48	4.7	19	69	4.1
7/20/2014	Summer	0.7	0.14	0.13	0.48	9.0	17	43	1.3
8/30/2014	Fall	10	0.39	0.12	0.60	14	50	118	2.4
9/2/2014	Fall	2.9	0.24	0.08	0.60	7.1	18	78	3.0
9/11/2014	Fall	8.6	0.34	0.18	2.04	17	38	136	2.2
10/6/2014	Fall	3.1	0.20	0.17	0.96	21	27	49	0.6
10/10/2014	Fall	2.3	0.26	0.05	0.72	8.1	22	100	3.4
10/14/2014	Fall	0.9	0.77	0.20	0.96	30	67	418	3.8
10/29/2014	Fall	13	0.27	0.05	0.24	7.4	22	167	6.3
11/17/2014	Fall	10	0.74	0.09	0.48	7.4	58	451	17

Table A.5. Physical and chemical characteristics of water samples at site SC1.

Date	Volume (m ³)	pH	TSS (mg/L)	VSS (mg/L)	NO ₂₊₃ -N (mg/L)	O-PO ₄ (µg/L)	SO ₄ (mg/L)	Total Coliform (CFU/100 mL)	Fecal Coliform (CFU/100 mL)
3/16/2014	528	7.97	72.0	19.0	0.38	ND ^a	5.19	–	–
3/29/2014	288	7.93	173	38.8	0.08	163	4.41	–	–
5/23/2014	50	8.61	36.9	12.5	1.09	80.3	7.31	93,000	19,000
5/25/2014	99	7.79	53.8	15.0	0.97	70.3	5.63	600,000	50,000
6/5/2014	105	7.63	50.6	11.9	0.39	135	5.20	311,000	42,000
8/2/2014	3,470	7.62	154	20.2	0.24	256	2.68	–	–
8/10/2014	510	7.77	58.8	16.9	–	–	–	118,000	24,000
8/20/2014	800	7.69	139	27.5	0.41	198	3.28	308,000	15,000
8/30/2014	556	7.66	124	25.6	0.21	91.3	2.32	263,000	60,000
9/2/2014	119	7.59	90.6	20.0	0.18	16.1	4.17	83,000	19,000
9/11/2014	466	7.67	45.0	10.6	–	–	–	173,000	25,000
10/10/2014	798	7.81	21.9	3.75	0.05	226	1.74	60,000	32,000
10/14/2014	2,161	8.01	55.0	13.1	0.19	88.3	2.26	–	–
11/17/2014	593	7.86	86.0	18.0	0.12	209	2.14	228,000	42,000

^aND, not detected.

Table A.6. SC1 rainfall and flow characteristics.

Date	Season	ADP (days)	P_t (in.)	I_{ave} (in/hr)	I_{max5} (in/hr)	Q_{ave} (l/s)	Q_{max5} (l/s)	V (m ³)	D_v (hr)
3/16/2014	Spring	13	0.47	0.06	0.20	9.1	78	528	16
3/29/2014	Spring	11	0.19	0.05	0.36	20	82	288	4.1
5/23/2014	Spring	7.7	0.12	1.44	1.44	10	24	51	1.4
5/25/2014	Spring	2.3	0.10	0.25	0.72	4.3	48	99	6.3
6/5/2014	Summer	0.7	0.20	0.16	1.20	50	72	105	0.6
8/2/2014	Summer	5.9	1.07	2.29	4.80	1,157	1,862	3,470	0.8
8/10/2014	Summer	2.0	0.23	0.49	0.72	123	166	510	1.1
8/20/2014	Summer	0.2	0.31	0.23	1.44	123	345	800	1.8
8/30/2014	Summer	10	0.39	0.12	0.60	42	190	556	3.7
9/2/2014	Fall	2.9	0.24	0.08	0.60	10	47	119	3.3
9/11/2014	Fall	8.6	0.34	0.18	2.04	54	107	466	2.4
10/10/2014	Fall	2.3	0.26	0.05	0.72	145	242	798	1.5
10/14/2014	Fall	0.9	0.77	0.20	0.96	225	358	2,161	2.7
11/17/2014	Fall	10	0.74	0.09	0.48	10	206	593	16

Table A.7. Physical and chemical characteristics of water samples at site SC2.

Date	Volume (m ³)	pH	TSS (mg/L)	VSS (mg/L)	NO ₂₊₃ -N (mg/L)	O-PO ₄ (µg/L)	SO ₄ (mg/L)	Total Coliform (CFU/100 mL)	Fecal Coliform (CFU/100 mL)
6/29/2014	1,705	8.15	51.3	16.3	0.38	8.11	4.75	55,000	10,000
7/18/2014	3,315	6.75	20.0	1.88	0.16	ND ^a	4.30	29,000	18,000
7/20/2014	2,100	7.59	15.0	2.50	0.34	ND	5.07	16,000	5,000
7/27/2014	5,640	7.49	266	50.6	0.40	ND	6.33	—	—
8/2/2014	4,994	7.53	198	27.5	0.15	ND	2.26	54,000	25,000
8/10/2014	2,897	7.76	38.8	13.8	0.38	ND	4.44	36,000	10,000
8/20/2014	1,980	7.53	55.7	12.1	0.29	ND	3.73	25,000	13,000
8/30/2014	3,800	7.90	97.5	23.8	0.14	ND	2.93	68,000	20,000
9/2/2014	3,265	7.94	23.8	8.75	0.20	ND	3.69	36,000	26,000
9/11/2014	3,111	7.84	111	23.8	—	—	—	32,000	23,000
10/6/2014	1,548	8.28	35.8	20.0	—	—	—	22,000	7,000
10/10/2014	9,693	7.80	50.0	8.75	0.10	28.2	1.94	39,000	13,000
10/14/2014	13,677	7.84	32.5	10.0	0.12	72.2	2.69	—	—
10/29/2014	3,824	7.76	6.67	3.33	0.48	ND	4.64	8,000	6,000
11/17/2014	10,358	7.74	92.5	20.5	0.13	ND	2.57	—	—

^aND, not detected.

Table A.8. SC2 rainfall and flow characteristics.

Date	Season	ADP (days)	P_t (in.)	I_{ave} (in/hr)	I_{max5} (in/hr)	Q_{ave} (l/s)	Q_{max5} (l/s)	V (m ³)	D_v (hr)
6/29/2014	Summer	2.8	0.27	0.15	0.60	128	327	1,705	3.7
7/18/2014	Summer	10	0.47	0.08	0.48	181	393	3,315	5.1
7/20/2014	Summer	0.7	0.22	0.13	0.48	240	529	2,100	2.4
7/27/2014	Summer	7.6	1.03	0.61	3.96	1,205	1,731	5,640	1.3
8/2/2014	Summer	5.9	1.28	2.29	4.80	1,342	2,172	4,994	1.0
8/10/2014	Summer	2.0	0.24	0.49	0.72	333	471	2,897	2.4
8/20/2014	Summer	0.2	0.26	0.23	1.44	393	739	1,980	1.4
8/30/2014	Summer	10	0.40	0.12	0.60	266	784	3,800	4.0
9/2/2014	Fall	2.9	0.35	0.08	0.60	161	316	3,265	5.6
9/11/2014	Fall	8.6	0.55	0.18	2.04	224	1,011	3,111	3.8
10/6/2014	Fall	3.1	0.19	0.17	0.96	159	306	1,548	2.7
10/10/2014	Fall	2.3	0.30	0.05	0.72	579	1,585	9,693	4.6
10/14/2014	Fall	0.9	0.82	0.20	0.96	942	1,446	13,678	4.0
10/29/2014	Fall	13	0.37	0.05	0.24	177	270	3,824	6.0
11/17/2014	Fall	10	0.83	0.09	0.48	389	1,093	10,358	7.4

Appendix B, Site photos



Figure B.1. Site RO2 security box, rain gage, and solar panel.



Figure B.2. Site SC1 sampling point.



Figure B.3. Site SC1 sampling point looking upstream through conveyance tunnel.



Figure B.4. Site SC2 sampling point.



Figure B.5. Site SC2, sampling point looking upstream.

Appendix C, Laboratory methodology

pH

Composite sample pH was measured in the laboratory using a Denver Instrument™ Model 250 pH, ISE, Conductivity Meter with the Denver Instrument™ pH/ATC electrode. The pH meter was standardized before each measurement with pH 4, 7, and 10 buffer solutions. It was rinsed with DI water and blotted dry using a Kim-wipe prior to each measurement. The probe was placed in the sample water and the pH was read when the meter reached the end cycle point indicated with a beep.

Suspended Solids

Total Suspended Solids

Total suspended solids were determined using Standard Method 2540D (APHA, 2005). The Millipore™ AP40 glass-fiber filter and the Millipore™ Chemical Duty Vacuum/Pressure Pump (115v, 60 Hz) filtration system were used. First, the glass-fiber filter disks were prepared. Each filter was placed on the vacuum apparatus, rinsed three times with 20 milliliters of DI water, ignited in an oven at 550°C for 15 minutes in order to measure volatile suspended solids, and placed in a desiccator until needed. At the time sampling, the filter was taken out of the desiccator and weighed. The filter was then placed on filtration apparatus and wetted with DI water to hold it in place. Volumes of 40 to 100 mL of the composite sample from each site was filtered. Each site was sampled twice to produce duplications. After each disk was suctioned, the beaker and filter apparatus was rinsed in triplicate with DI water to ensure no cross-contamination between sampling sites. Disk samples were dried in an oven at 103°C for 24

hours. After the drying period the filter disks were weighed and the calculation to determine concentration was as follows:

$$\begin{aligned} \text{total suspended solids, } mg/L \\ = \frac{[(\text{weight of filter} + \text{solids, g}) - (\text{weight of filter, g})] * 1000}{\text{sample volume filtered, mL}} \end{aligned}$$

(Equation C.1)

The final recorded EMC was determined by averaging the two duplicates.

Volatile Suspended Solids

Volatile suspended solids were determined using Standard Method 2540E (APHA, 2005).

The dry sample filters produced by 2540D were taken from the drying oven and weighed. The samples were then placed in a furnace and ignited at 550°C for 15 minutes, after which the samples were weighed again. Volatile suspended solid concentrations were determined using the following equation:

$$\begin{aligned} \text{volatile suspended solids, } mg/L \\ = \frac{\left[(\text{weight of filter} + \text{solids before ignition, g}) - (\text{weight of filter} + \text{solids after ignition, g}) \right] * 1000}{\text{sample volume filtered, mL}} \end{aligned}$$

(Equation C.2)

Indicator Microorganisms

Total coliform counts were determined using Standard Methods 9222B using a m-Endo medium. Fecal coliform counts were determined using Standard Methods 9222D using an mFC medium. Agar was prepared per the method and heated to near boiling to dissolve the agar. Volumes of 5- to 7-mL quantities were dispensed into 50-mm plastic petri dishes. Ideal sample size was achieved by pipetting multiple stormwater samples at various dilutions onto the petri

dish. Stormwater samples were analyzed in duplicate. Samples were then incubated for 22 to 24 hours at $35\pm0.5^{\circ}\text{C}$ for total coliforms, and a temperature of $44\pm0.5^{\circ}\text{C}$ for fecal coliform samples.

Nutrients

Nitrite (NO_2), nitrate (NO_3), ortho-phosphate (O-PO_4), and sulfate (SO_4) anions were determined by Standard Method 4110B (APHA, 2005). Samples were first filtered through the glass fiber filter disk used to determine suspended solids to remove particles larger than $0.45\text{ }\mu\text{m}$. The filtered sample were pipetted in duplicate into 3-ml glass vials for ion chromatography (IC) analysis. Samples were processed using either a Dionex AS-AP, ICS-2100, ICS-1100 depending on availability. Concentrations of each anion were determined by referring to the appropriate calibration curve after the IC system had come to equilibrium conditions. Calibration curves were determined by plotting multiple peak area verses concentration values and may be found in **Figures C-1 through C-4**. Nitrite plus nitrate as nitrogen was calculated by converting each constituent to the nitrogen equivalent and added together.

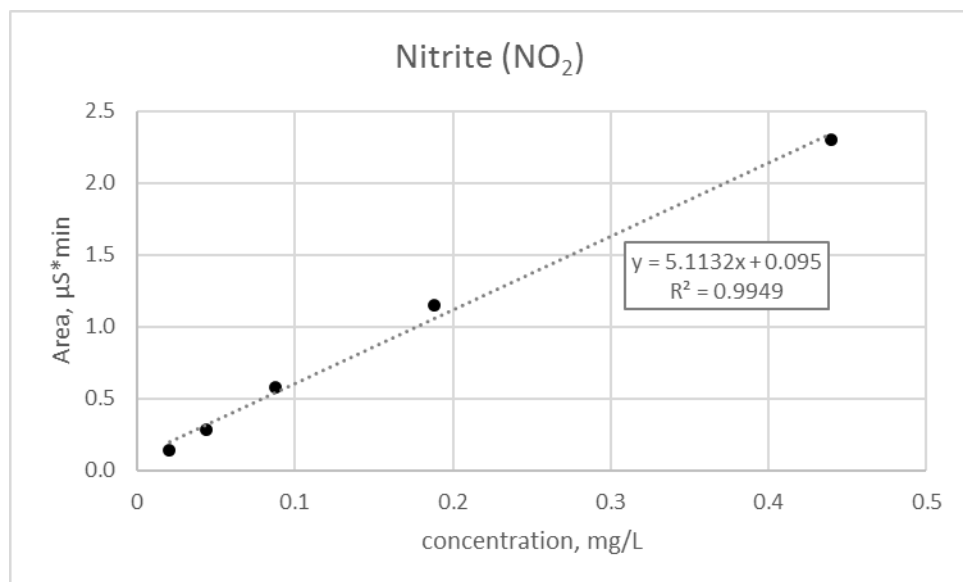


Figure C.1. Nitrite calibration curve.

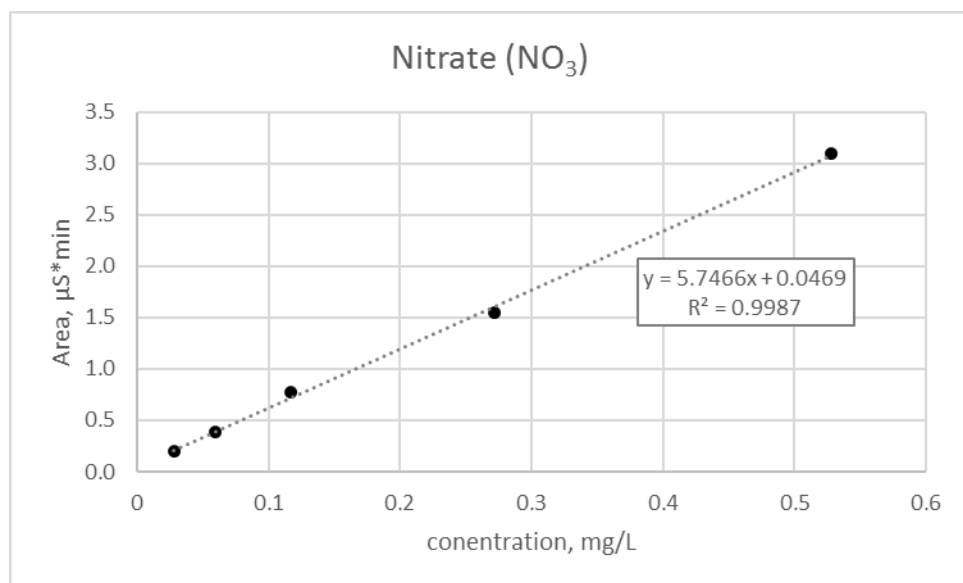


Figure C.2. Nitrate calibration curve.

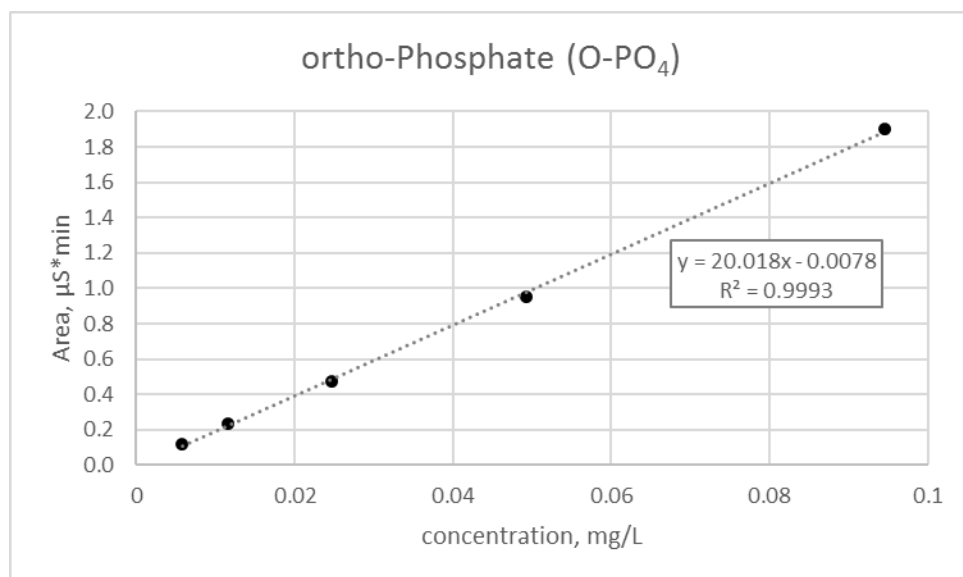


Figure C.3. Ortho-phosphate calibration curve.

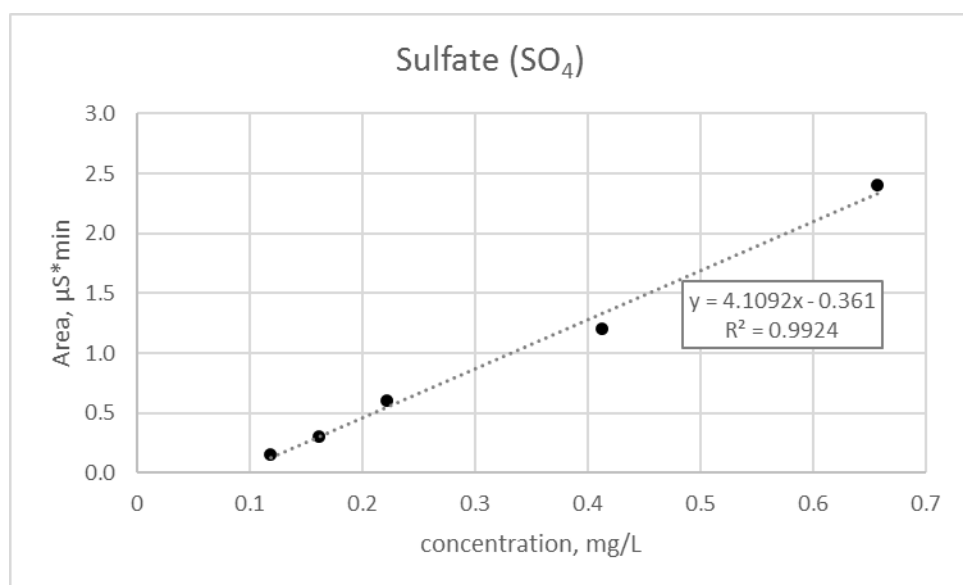


Figure C.4. Sulfate calibration curve.

Vita

Andrew Steinman was born in Omaha, NE on October 17, 1980. His family later moved to Gering, NE where he graduated high school from Gering High School in 1999. Following his high school graduation, he enlisted in the United States Navy, serving as a Corpsman. He served for five years, following two tours of duty in Virginia and Guantanamo Bay, Cuba before being honorably discharged in 2004. He spent the next 3 years pursuing his hobby of music and audio engineering. In 2007, he made the decision to change career paths and began pursuit of career in environmental engineering. In December of 2012, he graduated from the University of Tennessee, Cum laude, with a Bachelor of Science in Civil Engineering. In May 2017, Mr. Steinman will receive a Master of Science degree in Environmental Engineering with a concentration in Water Resources.